Design and Fabrication

of New Types of Micro Optical Components

A Thesis

In

The department

Of

Electrical and Computer Engineering

Presented in Partial Fulfillment of the Requirements

For the Degree of Master of Applied Science at

Concordia Uninversity

Montreal, Quebec, Canada

August 2004

@ Lijun Zhang, 2004

Library and Archives Canada

Published Heritage Branch

395 Wellington Street
Ottawa ON K1A 0N4
Canada

Bibliothèque et Archives Canada

Direction du Patrimoine de l'édition

395, rue Wellington
Ottawa ON K1A 0N4
Canada

Your file Votre référence
ISBN: 0-612-94719-X
Our file Notre référence
ISBN: 0-612-94719-X

The author has granted a non-exclusive license allowing the Library and Archives Canada to reproduce, loan, distribute or sell copies of this thesis in microform, paper or electronic formats.

L'auteur a accordé une licence non exclusive permettant à la Bibliothèque et Archives Canada de reproduire, prêter, distribuer ou vendre des copies de cette thèse sous la forme de microfiche/film, de reproduction sur papier ou sur format électronique.

The author retains ownership of the copyright in this thesis. Neither the thesis nor substantial extracts from it may be printed or otherwise reproduced without the author's permission.

L'auteur conserve la propriété du droit d'auteur qui protège cette thèse. Ni la thèse ni des extraits substantiels de celle-ci ne doivent être imprimés ou aturement reproduits sans son autorisation.

In compliance with the Canadian Privacy Act some supporting forms may have been removed from this thesis.

Conformément à la loi canadienne sur la protection de la vie privée, quelques formulaires secondaires ont été enlevés de cette thèse.

While these forms may be included in the document page count, their removal does not represent any loss of content from the thesis.

Bien que ces formulaires aient inclus dans la pagination, il n'y aura aucun contenu manquant.

Canada

Abstract

Design and Fabrication of New Types of Micro Optical Components

Lijun Zhang

Some novel micro planar optical components (MPOC) and a micro wire grid polarizer are designed and fabricated. As one of the application of MPOC, a device for color recognition is designed and fabricated.

Characteristics of mediums like light, silicon dioxide, silicon and polysilicon as well as their interactions with light are discussed. Making use of the theory of optical physics and geometrical optics, the principle of light path control components and the properties of light energy transmission are analyzed. Power loss of MPOC is simulated by specific optics software. Micro wire grid polarizer is designed and fabricated using MUMP technologies with the support of Canadian Microelectronic Corporation (CMC). Different from traditional optical components fabrication process, the fabrication process coming from chip fabrication technology is applied for the first time for making MPOC. Fabrication of MPOC is conducted in micro-fabrication laboratories at Concordia. All devices are fabricated in micron scales and are compatible with optical fibre light coupling.

The processes employed here for fabrication of the micro optical components can greatly reduce the components dimensions and decrease the production cost by a mass production supported by the process.

Acknowledgement

I hereby express my sincere thanks to Dr. Mojtaba Kahrizi of Electrical and Computer Engineering Department, for his continual and devoting instructions during the whole project.

I also thank Mr. Bowei Zhang for his help in optical fiber instrument operation, Mr. Jun Chen for his help in doing some experiments, Mr. Xiaohong Mu and Mr. Siamak Fouladi for their helps in MEMPs PRO application, I also thank all the others who ever gave me their kind help during the project.

Content

List of Figures

List of Tables

Chapter 1 Introduction and Background

Section 1.1 Light and Material

Light

Light had been proved to be of the electromagnetic nature [1]. The existence of electromagnetic waves followed from the set of equations that Maxwell proposed in 1861 which adequately describe high frequency alternating electromagnetic fields, including optical waves, as well as the theory of interaction of light and matter. They may be written in the Gaussian system of units (which is convenient for optics) as

$$rot\vec{H} = \frac{1}{c}\frac{\partial \vec{H}}{\partial t} \qquad 1$$

$$rot\vec{E} = -\frac{1}{c}\frac{\partial \vec{H}}{\partial t} \qquad 2$$

$$div\vec{E} = 0 \qquad 3$$

$$div\vec{H} = 0 \qquad 4$$

Here E and H are the strengths of electric and magnetic fields and c is the electro-dynamic constant, equal to the velocity of light in vacuum.

Researches indicate that the radiation properties of light are close to that of plane or spherical harmonic waves. Mathematically speaking, any arbitrary optical field may be a superposition of standard waves and is possible to be decomposed in to a spectrum, which means to perform spectral expansion that performed in current

optical experiments. Moreover, spectral expansions are capable of being generalized to wave beams, i.e. to spatially modulated waves treated as a superposition of plane waves propagating in various directions. The energy flux brought by an optical wave is described by Maxwell theory. The intensity I and the complex amplitude E of the wave have such relations as follows

$$I = \frac{c}{8\pi} |E|^2 \qquad 5$$

$$\vec{E} = \frac{1}{2} E \exp[i(\omega t - kz)] + c.c \qquad 6$$

These formulae are valid for a plane monochromatic optical wave propagating in the vacuum. From the equations, we may notice that the electric field intensity varies with frequency and spatial position of propagation.

In terms of wavelength, among the whole spectrum, the visible spectrum ranges from 400nm violet light to 760nm red light.

Visible light	Wavelength
Red light	625 nm---740nm
Green light	520 nm-- 565nm
Blue light	435 nm---500nm

Table1. Wavelength range of three primary color

A light wave is an electromagnetic wave which travels through the vacuum of outer space. An electromagnetic wave is a transverse wave which has both an electric and a magnetic component.

A light wave which is vibrating in more than one plane is referred to as unpolarized light [2]. Such light waves are created by electric charge which vibrates

in a variety of directions, thus creating an electromagnetic wave which vibrates in a variety of directions. In general, unpolarized light is regarded as a wave which has an average of half its vibrations in a horizontal plane and half of its vibrations in a vertical plane.

Unpolarized light can be transformed into polarized light. Polarized light waves are light waves in which the vibrations occur in a single plane. The process of transforming unpolarized light into polarized light is known as polarization. There are a variety of methods of polarizing light, for example, polarization by transmission, by reflection, by refraction, and by scattering.

The most common method of polarization involves the use of wire grid polarizer (WGP). WGP are made of a conductive material. It is capable of blocking one of the two planes of vibration of an electromagnetic wave. When unpolarized light is transmitted through a WGP, it emerges with one-half the intensity and with vibrations in a single plane; it emerges as polarized light.

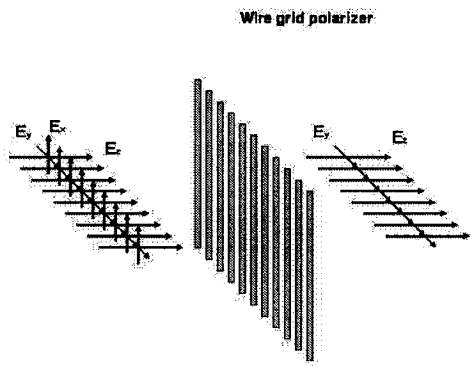

Figure 1 Principle of wire grid polarizer

As unpolarized light strikes the filter, the electromagnetic vibrations which are in a direction parallel to the alignment of the molecules are absorbed.

Silicon

Si as an important semiconductor material is widely used in electronic devices and in recent years, its special structure has played an important role in the new technology called MEMS.

The application of Si in MEMS comes from its anisotropic feather with single crystal structure. It has regular geometric periodicity throughout the entire volume of the material. The periodic arrangement of atoms in the crystal is called the lattice which constructs diamond structure.

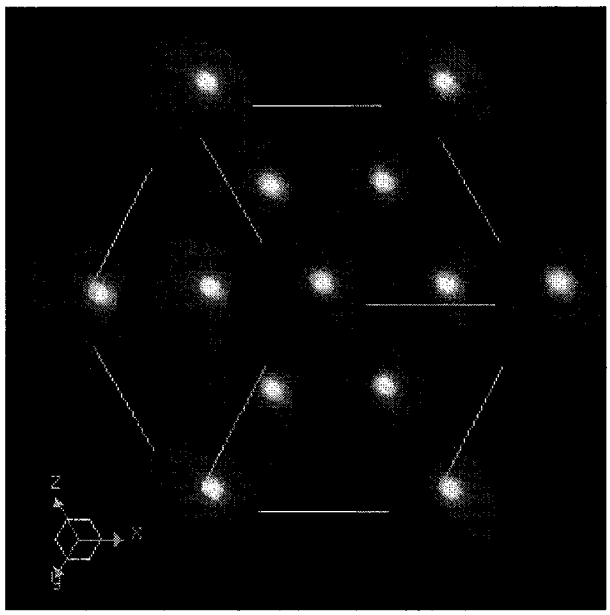

Fig.2 Si structure

The structure is basically a body-centered cubic with four of the corner atoms missing. Every atom in the tetrahedral structure has four nearest neighbours and it is this structure which is the basic building block of the diamond lattice.

Silicon Dioxide

SiO_2 is an amorphous, inorganic, transparent or translucent optical material which is called glass. When passing through SiO_2, light would be diffused. In practical, this material is always doped with some special particles, giving rise to mixture. Just for this, the various type of optical glass get their different characteristics, for instance, different refractive index, from the many different combinations of ingredients mixed together.

When glass is made with pure silicon dioxide (SiO_2), and with no addictive, the resulting glass type is known as fused silica. After being oxidized, Si wafer surface has fuse silica layer. Some other groups of glasses include alkali silicate, soda-lime, borosilicate, and lead glass group.

In general, there are some physical imperfections in glasses [2]. Striae is the term for the lines seen in the glass that is the result of incomplete mixing of the ingredients when the glass is melted. Stones, as the name implies, are the result of foreign matters and/or of incomplete melting of earthen materials when the glass is made. These imperfections make the light wave decay during its propagation through the glass. Moreover, stress in SiO_2 also influence light transmission performance.

Poly silicon

Thin films of polycrystalline silicon, or polysilicon are widely used as microelectronic products[3]. It is usually deposited by thermal decomposition or pyrolysis of silane at temperature from 580-650 degrees centigrade.

Poly-Si is compatible with high temperature processing and interfaces very well with thermal SiO_2. Besides, the electrical characteristics of poly-Si thin film

depend on its doping level. Heavily-doped poly thin films can be used in emitter structures in bipolar circuits.

Common dopants for polysilicon include arsenic, phosphorus, and boron. Polysilicon is usually deposited undoped, with the dopants just introduced later on after deposition.

Section 1.2 Interaction between light and SiO_2

Like vacuum, SiO_2 is homogeneous medium allowing rectilinear propagation of light in it with constant velocity. This rectilinear propagation characteristic of light is fundamental postulate of geometrical optics.

However, when light from air encounters a medium surface like glass, the speed of light slow down, accompanying the change of propagation direction. As the light gets out of the glass and travels into the air again, it regains that velocity when it is in air. Resulting from the different speed of light inside and outside one medium, a term called index of refraction is defined by the ratio of the speed of light in a vacuum to the speed of light in the medium, as shown below:

$$n = v_0 / v_1 \qquad 7$$

Where v_0 is the speed of light in vacuum, v_1 is the speed of light in the medium. v_1 is not the same constant for all the wavelength of light in same medium, in fact. Therefore it cause the refractive index varies with the different wavelength and different change of propagation direction regarding to light with different wavelength. The relation between wavelength and refractive index is shown as Figure 3.

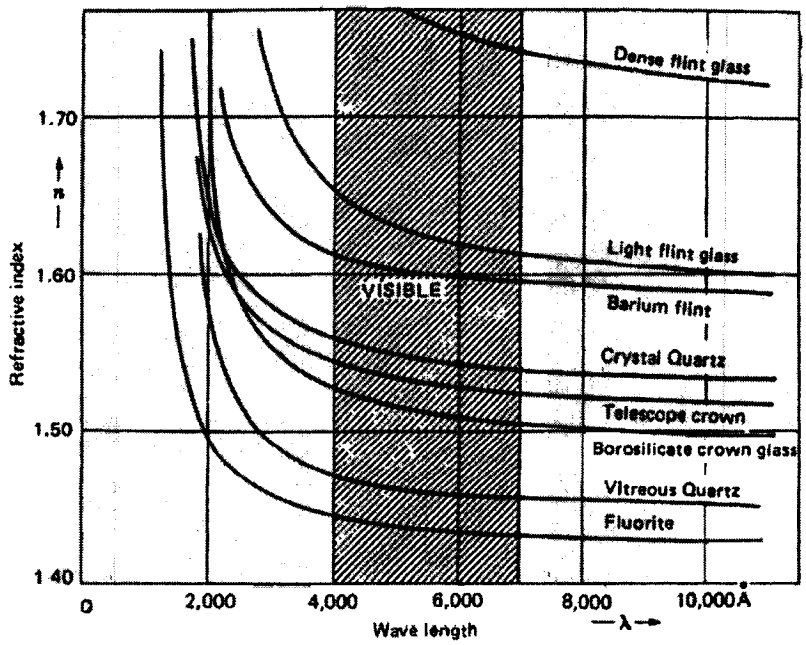

Figure 3 Refractive index vs wavelength

In noncrystalline materials, the refractive index is isotropic, that means the refractive index does not depend on the direction. That is to say, noncrystalline solid such as glass and liquids are optically isotropic. This guarantee that light may keep its rectilinear propagation in such medium.

When light propagates through SiO_2, it becomes attenuated in the direction of propagation because of absorption and scattering, which give rise to a loss of intensity in the regular direction of propagation. One example of absorption attenuation is called lattice absorption, which the absorbed energy peaks when the frequency of the wave is close to the natural lattice vibration frequencies. The other example of scattering attenuation is termed Rayleigh scattering. In this type of attenuation, the particle size is typically smaller than one-tenth of the wavelength.

Rectilinear propagation of light will change its direction when it go out of one medium into another different medium. This is represented by different deviation

from the direction of light propagation, of different frequencies in the light, after the change of light propagating medium. The value of deviation may be calculated by Snell's law.

A beam of light incident on a boundary between two different optical medium normally splits into two beams transmitting to two directions, one continuing on propagating forward through the medium it encountered and being refracted, the other turning and reflecting back to the original medium. The performances of the refracted and reflected beams, such as the propagation direction, and power, based on the both composition of both medium and on the parameters of the incident beams such as its direction, frequency, and power. In terms of quantity, this phenomenon can be expressed by Fresnel formulae. By taking advantage of these properties of reflection and refraction, light-controlling instruments (e.g. lenses, prisms, mirrors, etc) are successfully made to focus light, perform spectral decomposition of light, and so on.

To describe the relation for reflection and refraction of a light at the boundary of two different medium, Fresnel's Formulae gives a reasonable description in terms of energy.

Assume that the incident, reflected and refracted optical waves are plane wave and monochromatic. The two mediums which form the boundary between them are to be linear and isotropic.

The characteristics of light propagation in both medium is described

$$\vec{E} = \frac{1}{2}\vec{\varepsilon}\ \exp[\ \ i(\omega t - \vec{k}\vec{r})] + c.c., \qquad 8$$

$$\vec{H} = \frac{1}{2}\vec{h}\ \exp[\ \ i(\omega t - \vec{k}\vec{r})] + c.c., \qquad 9$$

$$\vec{D} = \frac{1}{2}\vec{d}\ \exp[\ \ i(\omega t - \vec{k}\vec{r})] + c.c., \qquad 10$$

Fresnel formulae establish the relationship between the amplitudes of the incident, and reflected optical waves.

$$r_{\perp} = \frac{\sin(\theta_1 - \theta_2)}{\sin(\theta_1 + \theta_2)} \qquad r_{//} = -\frac{\tan(\theta_1 - \theta_2)}{\tan(\theta_1 + \theta_2)} \qquad 11$$

These equations illustrate that only part of the light energy may enter into another medium because of the interaction between light and medium.

When the sum of the angles of incidence and refraction is equal to $\theta 1+\theta 2=\pi/2$ $r_{//} = 0$, means the reflected light disappeared. This phenomenon is called the Brewster effect. At this time, the angle of incidence is called the Brewter Angle, is

$$\theta_B = \arctan(n_2 / n_1)$$

According to Eq.11, if $\theta_1=0$, then the above equation can be changed into

$$r_{\perp} = -\frac{n_2 - n_1}{n_1 + n_2} \qquad r_{//} = \frac{n_2 - n_1}{n_1 + n_2} \qquad 12$$

As Brewster effect exists, when light encounters another medium, it is possible not to refract into the medium. Specifically, in order to couple light into optical fibre, only rays which are made falling within a certain cone at the input of the fibre can normally be propagated through the fibre. Other rays would be refracted into cladding, which result in light signal attenuation. Figure 4 shows the path of a light ray launched from the outside medium of refractive index n_0 (not necessarily air) into the fibre core.

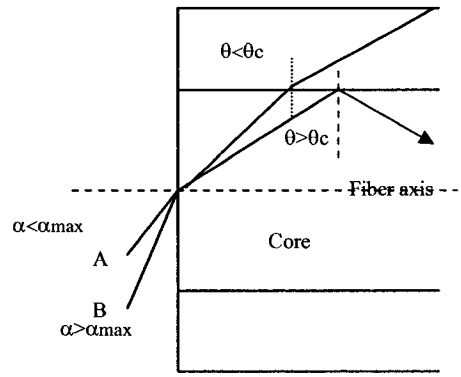

Figure 4 Numerical aperture

Suppose that the incidence angle at the end of the fibre core is α, and inside the waveguide the ray makes an angle θ with the normal to the fibre axis. Then unless the angle θ is greater than the critical angle θ_c for TIR, the ray will escape into the cladding. Thus, for light propagation, the launching angle α has to meet the demand that TIR is supported within the fibre.

The numerical aperture NA is a characteristic parameter of an optical fibre

$$NA=(n_1^2-n_2^2)^{1/2}$$

defined by refractive indexes. So that in terms of NA, the maximum acceptance angle, α_{max} becomes,

$$\sin\alpha_{max}=\frac{NA}{n_0} \qquad 13$$

The angle 2 α_{max} is called the total acceptance angle.

Section 1.3 Light path controlling optical components and polarizer

There are a lot of light path controlling components nowadays, but the most fundamental ones are lens, prism, and mirrors. They are playing a variety role in our

life, here we will discuss how the micro optical components work to select particular wavelength.

Lens

Referring to Fig.5, there is a spherical surface with radius r, separating two homogeneous medium with refractive index n and n′. The point L is located on the left side of the surface, if point O is set at the original, the coordinate of L is (x_1,y_1), the point L′ on its right, which coordinate is (x_2,y_2).

As both medium are homogeneous, the optical path consists of two straight lines segments LA and AL′. The optical path is n times the length LA plus n′ times length AL′. This quantity must be stationary relative to small motions of A along the surface, the only degree of freedom available. Using the notation indicated in Fig.5, we can write for the optical path

$$p(h) = n\sqrt{(x_1 + d)^2 + (h - y_1)^2} + n'\sqrt{(x_2 - d)^2 + (h - y_2)^2} \qquad 14$$

in which

$$d = r - \sqrt{r^2 - h^2}. \qquad 15$$

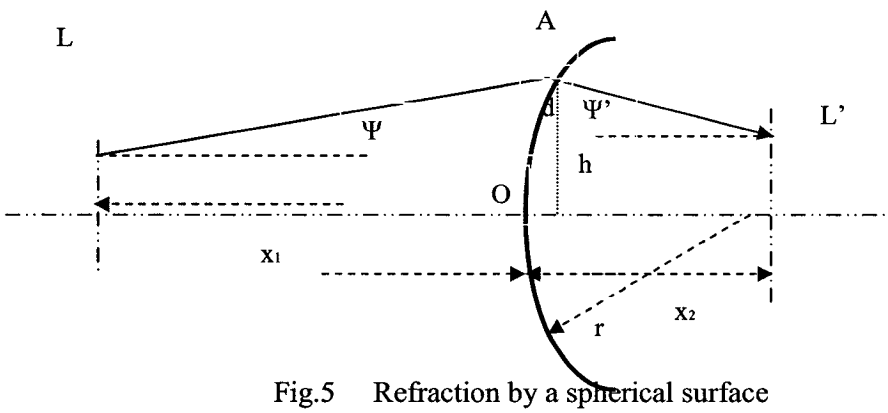

Fig.5 Refraction by a spherical surface

The function p(h) must be stationary in h. To get to the heart of the matter with as little mathematical baggage as possible, let us assume that y_1, h, and y_2 are small relative to r, p, and q, so that the quadratic terms in the series development of p(h) suffice. These terms can be found by using the approximation $\sqrt{1+\varepsilon} \cong 1+\varepsilon/2$. For the sag s we find $h^2/2r$, and for the path function E(h) we can write, after some rearranging:

$$p(h) = C_1 + C_2 * h + C_3 * h^2 \qquad 16$$

in which

$$C_1 = n * x_1 + n' * x_2 + \frac{n * (y_1)^2}{2 * x_1} + \frac{n'(y_2)^2}{2 * x_2}, \qquad 17$$

$$C_2 = -\frac{n * y_1}{x_1} - \frac{n' * y_2}{x_2}, \qquad 18$$

$$C_3 = \frac{1}{2}\left(\frac{n}{x_1} + \frac{n'}{x_2} - \frac{n'-n}{r}\right). \qquad 19$$

Eq.16 shows that p(h) is stationary in h when $C_2+2*C_1*h=0$. This relation can be rearranged into the form

$$n'\frac{y_2 - h}{x_2} = n\frac{h - y_1}{x_1} - h\frac{n'-n}{r} \qquad 20$$

As we have restricted ourselves to the small angle approximation, the first two fractions may be identified with the angle ψ' and ψ between the ray and the axis to the right and to the left of the surface. Note that $\psi'<0$ in Fig.5. The equation for h now takes the form

$$n'\psi' = n\psi - h\frac{n'-n}{r}. \qquad 21$$

The derivation appears straightforward, but there can be complications. Consider, for instance, a case in which x_1 and x_2 are chosen such that the constant C_3

is zero. No ray can travel between L and L'. An exception occurs y_1 and y_2 are chosen to make the constant C_2 zero as well. In that case p(h) is independent of h, i.e. the optical path function is stationary for every value of h. This suggests that in this very special case any ray departing from L will, after traveling the refracting surface, pass through the point L'.

These inclusions are, in fact, correct. If C_2 and C_3 are both zero, the point L is imaged at the point of L', i.e. all rays emanating from L arrive after refraction at point L'. The equation $C_3=0$ can be written in the form

$$\frac{n}{x_1}+\frac{n'}{x_2}=\frac{n'-n}{r} \qquad 22$$

which is the well known "lens maker formula"

According to this formula, it is very obvious that the performance of lens is subject to the medium properties, which are the refractive indexes of both side of the boundary, as well as geometric dimensions.

Prism

When rays pass through a prism, it will deviate from its original direction by a certain angle. This deviation angle may be calculated by determining angular dispersion of the prism.

As shown in the following Figure 6, when incident light AB encounter with the boundary of the prism, it will be refracted to travel along the path BC, then at the other boundary, the light is refracted again and travel along CD path. Therefore, the original incident light has been changed its direction two times after passing through the prism, in other words, it has been deviated. The deviation angle between AB and CD is represented by δ.

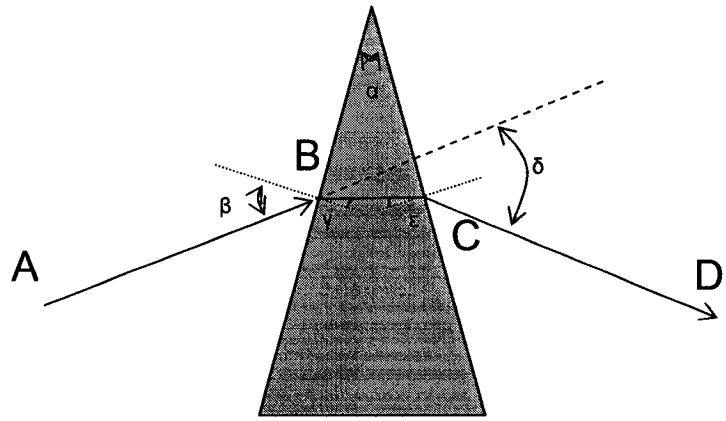

Figure 6 dispersion of the prism

The angular dispersion is a parameter which shows how much a prism separates light with different wavelength from each other. Its quantity is determined by both geometry and material dispersion, that is,

$$\frac{d\delta}{d\lambda} = \frac{d\delta}{dn}\frac{dn}{d\lambda} \tag{23}$$

where the geometrical contribution has the form

$$\frac{d\delta}{dn} = \frac{\sin\alpha}{\cos\gamma\cos\delta} \tag{24}$$

Where α is the apex angle of the prism and γ is the angle of refraction. Therefore, the angular dispersion for a prism is

$$\frac{d\delta}{d\lambda} = \frac{\sin\alpha}{\cos\gamma\cos\delta} * \frac{dn}{d\lambda} \tag{25}$$

In order to determine the value of dispersion, it is necessary to get the refractive index function, n(λ) [4]. In practice, dn/dλ is approximately equal to

$$\frac{\Delta n}{\Delta\lambda} = \frac{n_F - n_c}{\lambda_F - \lambda_c} \approx \frac{dn}{d\lambda} \tag{26}$$

Mirror

The principle of light reflecting off a curved surface is similar to that of light reflecting off a flat mirror which is on the position of the section of the spherical mirror. A spherical mirror is simply a piece cut out of a reflective sphere. It has a center of curvature, C, which corresponds to the center of the sphere it was cut from; a radius of curvature, r, which corresponds to the radius of the sphere; and a focal point where parallel light rays are concentrated on.

Spherical mirrors are either concave (diverging) mirrors or convex (converging) mirrors. In this design, convex spherical mirrors will be applied.

To determine where the ray path of the reflected light, it is very helpful to draw a ray diagram as follows

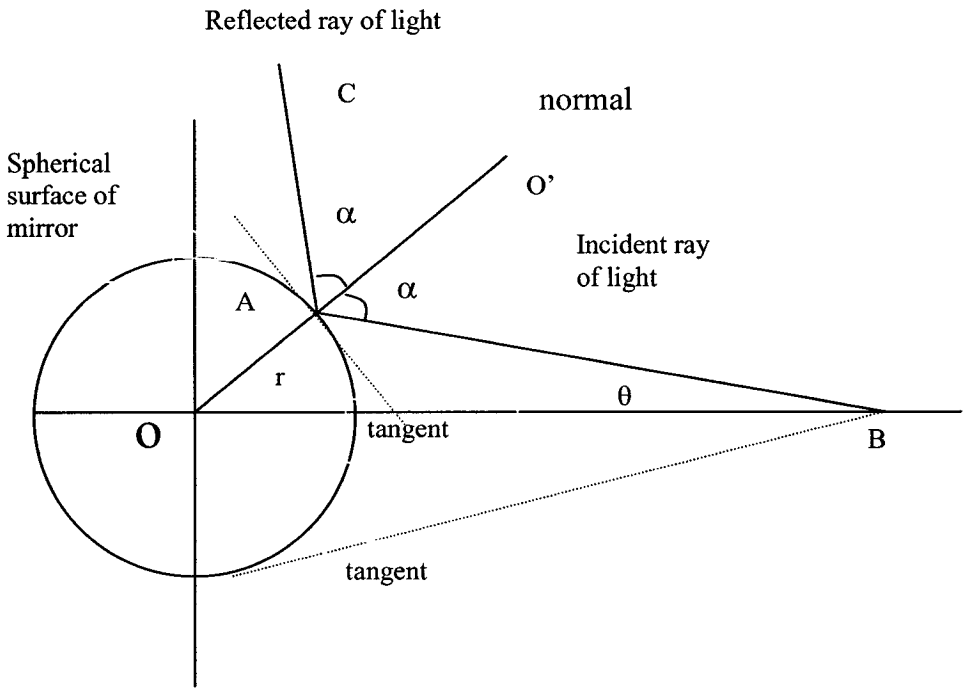

Figure 7 Ray tracing for a spherical mirror

From the diagram, we may see that the angles of the incident ray of light with the normal and that of reflected ray of light with the normal are the same. According to the relationships among the angles, the position of point B, as well as the radius of the spherical mirror, the precise equation for the reflected ray may be established.

Polarization characteristic of light

A propagating electromagnetic wave has its electric and magnetic field at right angles to the direction of propagation. If the direction of propagation is set as z-axis, the electric field can be in any direction in the plane perpendicular to the z-axis. When a beam of light has waves with the E field in each in a random direction but perpendicular to z, then the light is called unpolarized light

If the electric field components Ex and Ey of light are place on arbitrary pointed x and y axes, both E_x and E_y can be described respectively by a wave equation as follows:

$$E_x = E_{x0}\cos(\omega t - kz)$$

And $$E_y = E_{y0}\cos(\omega t - kz + \phi)$$

Where ω is the frequency of the light wave, Φ is the phase difference between Ey and Ex.

If E_{x0}=E_{y0} and Φ= 180 deg or Φ= -180 deg, the EM will be called linearly polarized light wave which the oscillation of the electric field are always contained within a line at an angle of 45 deg with x-axis.

If E_{x0}=E_{y0} and Φ= 90 deg or Φ= -90 deg, the EM will be called right circularly and left circularly polarized light waves, respectively.

If E_{x0} is not equal to E_{y0} and Φ is not zero or any multiple of 180 deg, the wave will be an elliptically polarized light wave.

Under certain circumstance, when unpolarized light interact with some materials, some of its energy in certain direction are absorbed or reflected, whereas in other directions, those light components are not significantly influenced.

Chapter 2 covers simulation and analytical results; chapter 3 discusses design and fabrication. Discussion and conclusion is followed in chapter 4.

Chapter 2 Simulation and Analytical Results

Section 2.1 Lens power loss simulation

In the simulation, we should set some parameters in advance. The wavelength of the incident light is set at 500nm, the refractive index of SiO_2 is 1.465, the refractive index of air is set to 1, the input power of the incident light is set to unit 1, and simulation result is the ratio of the output power to the input power. If setting the radius of both the front and the back surface are r, and the thickness of the lens is t. Assume the power loss in the air is 0

In the following figures, the contour map shows the shape of the component and the position of the detector, as well as the route that the light passes and its reflection and its refraction. With regard to the curve, the y-coordinate refers to the monitor value which in fact is the ratio of the output light power to the input light power; the x-coordinator refers to the time for the testing. C refers to light velocity in vacuum.

In the following graphs of simulation Fig.8, the thickness of the lens is set to 0, the front and back radius vary from 40μm to 160 μm, the contour maps show the light route and intensity variation, and the source locates at the center of bottom line under the lens. The detector is put at the other side of the lens. The curve gotten after simulation is the relationship between simulation time and the ratio of output to the input light power.

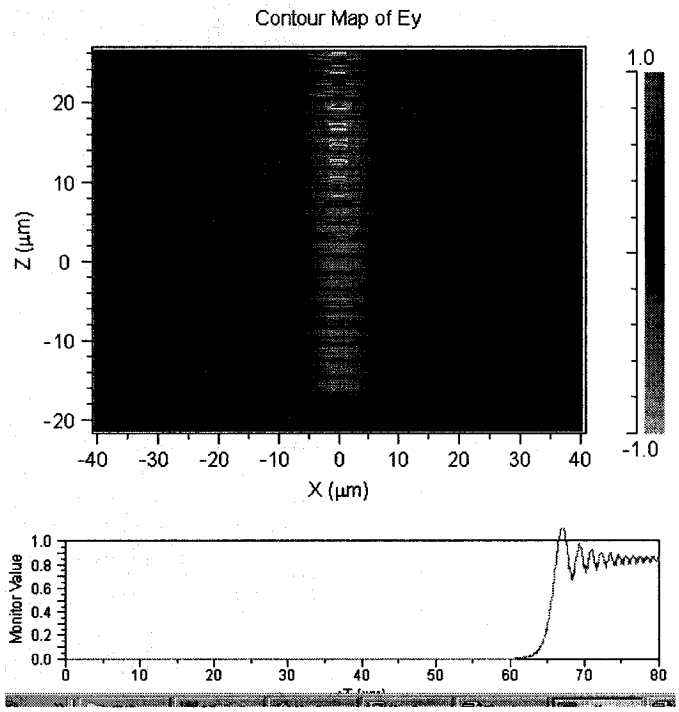

Figure 8 Waveform of the power loss ratio (r=40μm t=0)

From the above simulation results, we may get the relationship curve between the power loss with respect to the radius of the lens.

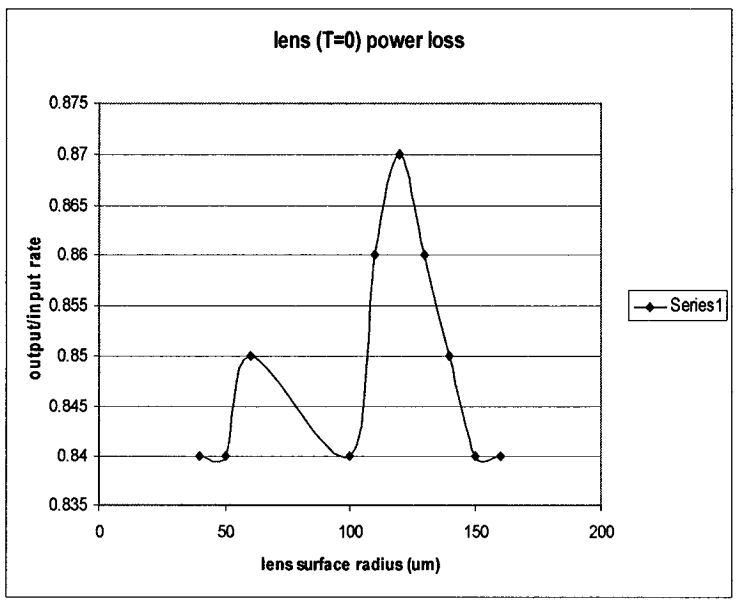

Fig.9 Waveform of the power loss ratio of the lens

From the figure above, we may see the power loss rate of the lens tested vary between the range of 0.84 to 0.87 when the front and back surface radius vary from 40 μm to 160μm and the thickness of the lens is 0.

For other figures, refer to appendix 1.

Section 2.2 Prism power loss simulation

When making simulation for prisms, we made tests at two different wavelength, respectively. One is at 500 nm, and the other is at 700nm, in order to see if there is much difference between different wavelengths in terms of power loss ratio.

Simulation at wavelength of 500nm

"A" refers to apex angle. "I" refers to incident angle.

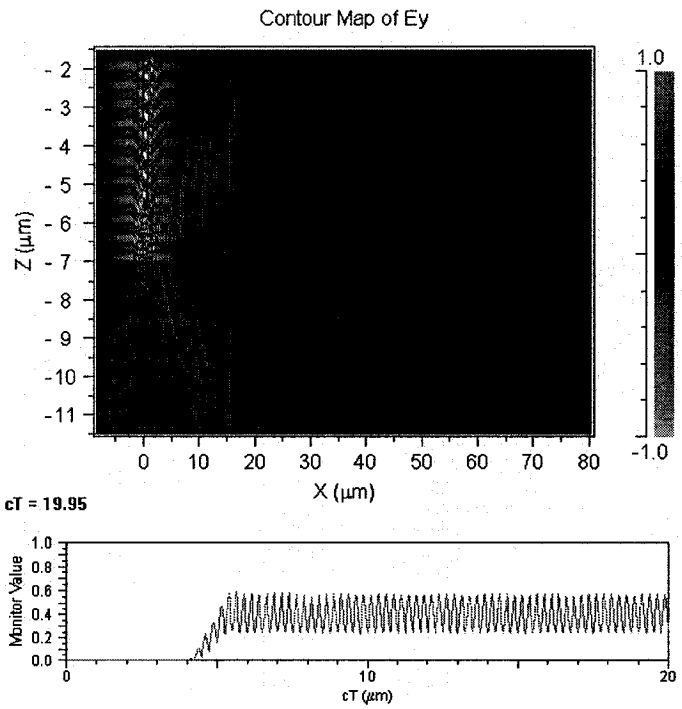

Figure 10 Waveform of power loss ratio of prism with A=15 deg.

I=40 deg.

Summarize from the above simulation graphs, we may get the following diagrams with regard to the relationships between power loss and incident angle.

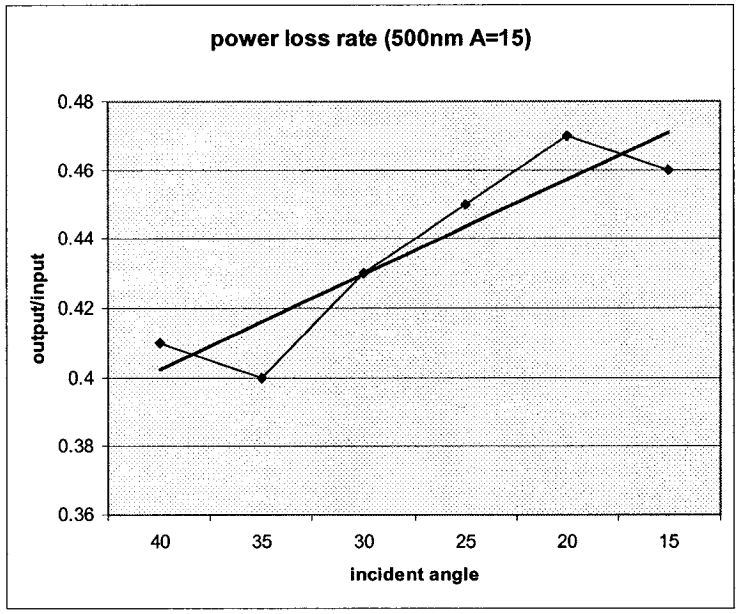

Figure 11 Waveform of power loss rate when A=15

For other figures, refer to appendix 1.

Analysis: When apex angles are 15, 30, and 40, respectively, the power loss rate vary from 0.47 to 0.4. The maximum of the rate happened at apex angle=15 deg. incident angle=20 deg.

In order to get more power output, we need to choose apex angle around 15-30 deg.

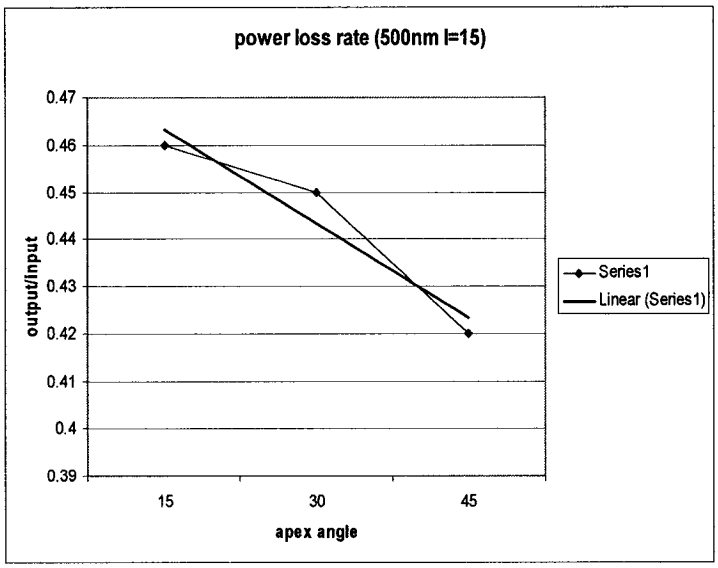

Figure 12 Waveform of power loss when I=15

Analysis of the above forms: when the incident angle I is determined, the power loss rate with regard to the apex angles tend to get smaller when the apex angles increase. In most cases, rate will range from 0.34 to 0.44. However, when I=15 deg, the rate gets down rapidly when the apex angle is larger than 30 deg. This is because the light approaches to the surface at nearly the critical angle so that the light can not pass the prism as usual.

For other figures, refer to appendix 1.

Simulation of power loss at wavelength 700nm

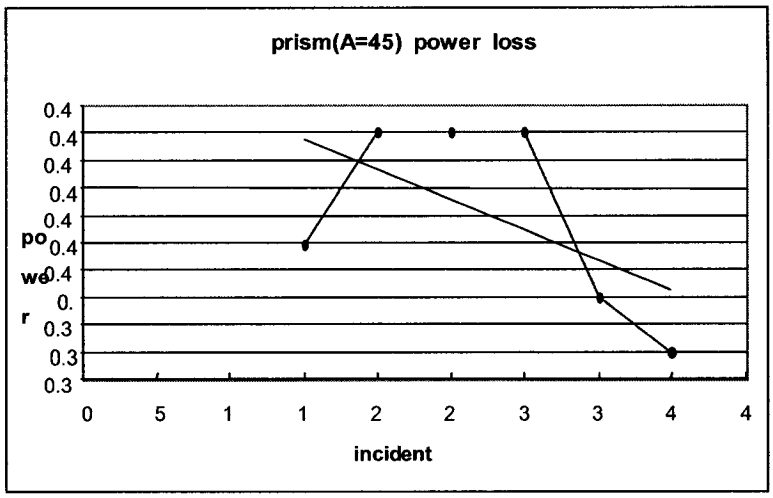

Figure 13 Waveform of power loss rate of prism when A=45 deg

Refer to appendix 1 to see other figures.

Analysis: When the apex angle has been determined, the power loss rate varies from 0.39 to 0.43. Only when the incident angle is more than 35 deg, two values of the power loss are less than 0.4.

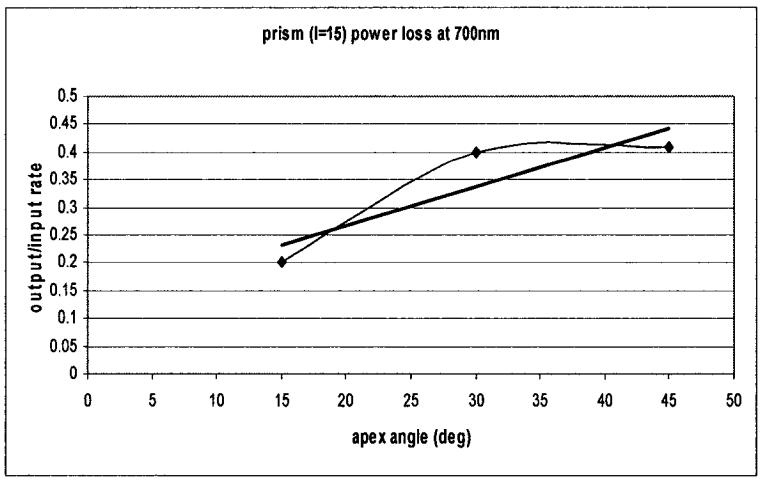

Figure 14 Waveform of the power loss rate when I=15 deg

For other figures, refer to appendix 1.

Analysis: In general, when the incident angle has been determined, the power loss ratios decrease slowly with the increase of the apex angle. But when the incident angle is near TRA, the ratio decrease rapidly when the apex angle increase. So in

order to get large output power, the incident angle should be around 15-40 deg.

In terms of the value of the ratio, both lights of 500nm and of 700nm are similar. The ratio generally inflates around 0.4 and no significant sign shows that the ratio has relationship with wavelength of light.

In terms of apex angle of the prism, as well as the incident angle, in the range from 15 deg. to 40 deg., the value of power loss ratio does not change significantly with change of the apex angle and the incident angle of light. This gives us more choices in choosing the geometric parameters of the prism.

Section 2.3 Analysis of power loss

Attenuation of power in the medium and between components is inevitable but can be decreased to minimum level if proper measures are taken. Before this, the mechanism of power loss should be mentioned and therefore actions for maintaining power transmitted may be conducted.

1. Defects in the medium

   In case that bubbles and striae, regions where the optical properties differ slightly from those of the bulk material, exist in the SiO_2 layer, the light travel will be interfered [5].

2. Absorption and scattering losses [6] are inborn causes of attenuation.
3. Roughness of the surface of optical components.

   The power loss due to roughness of the component surface may be decreased by using anti-reflecting and/or reflecting coatings.

4. Optical component edge should be perpendicular to the surface of the substrate. Otherwise, part of the light would be reflected upward or downward and is lost.

In terms of Geometric Optic, to realize the function of the device, what should do is just to make ray tracing and separate the desired light with particular wavelength from others. In fact, this is not enough, because light has different amount of loss in different path of ray. Some paths are not available for light signal to pass and reach the output terminal as the power of the light signal has been attenuated during transmission in those paths. Referring to the simulation results, it is easy to make a choice of the optical path by selecting one path which has higher ratio of output power to input power of the signal.

(End of Chapter 2)

Next chapter will introduce:

Chapter 3 Design and Fabrication

Section 3.1 Design of Micro optical components

Section 3.2 Fabrication of Micro optical components

Chapter 4 Discussion and Conclusion

Discussion of the 2 fabricated device

Conclusion

Chapter 3 Design and Fabrication

Section 3.1 Design of Micro optical components

Determination of refractive index

As the Figure 3 shown, the refractive index of the materials except light flint glass varies with the wavelength in nearly fixed rate in visible spectrum. Then assume the refractive index of fused silica varies with the wavelength in the same rate, if we measure refractive index of fused silica at a particular wavelength in visible spectrum, we may get similar curve for fused silica and get to know the refractive index at each particular wavelength in visible spectrum. At 6330 Å, the refractive index of SiO_2 layer is measured 1.377,

Studying the curve of Borosilicate crown glass, when wavelength varies from 4000Å to 6900 Å, the refractive index changes from 1.525 to 1.505, then the change rate Δ is: Rate $\Delta=(1.525-1.505) / (4000-6900) = -6.90\times10^{-6}$

Then the refractive index at wavelength of 6250Å will be:

$1.377+ (6250-6330) * (-6.9\times10^{-6}) =1.377 +0.00055=1.3776$

and the refractive index at wavelength of 7400 Å will be:

$1.377+ (7400-6330) * (-6.9\times10^{-6}) =1.377-0.007=1.370$

Lens design

In this device, the lens will be used to collimate rays of light, to focus the rays of lights out of the dispersive component, the prism, to select the wavelength we need, and to couple light signals into the waveguides.

According to optics theory, the parallel light incident to a convex lens will concentrate on the focus point of the lens, and rays of light come from the focus point of the lens will collimate at the other side of the lens. So we have to get the focus length of the lens.

The focus length has relations with the material properties, the geometric dimensions of the lens. This may be illustrated by the lens' maker equation.

In the previous discussion, lens maker equation is derived by the situation that light enters into another medium with curve surface. Considering lens which has two curve surfaces, the lens equation will be expressed as follows

$$\frac{1}{f} = (n_1'-1)[\frac{1}{r_1} - \frac{1}{r_2} + \frac{(n_1'-1)t_1'}{n_1' r_1 r_2} \qquad 23$$

Where f is the focal length, n_1' is the refractive index of the SiO_2, r_1 and r_2 are radius of the front and back surfaces of the lens, respectively.

Concerning the lens design, we use Matlab to make program to get the relations among the focal length and the geometric parameters of the lens, as well as material properties.

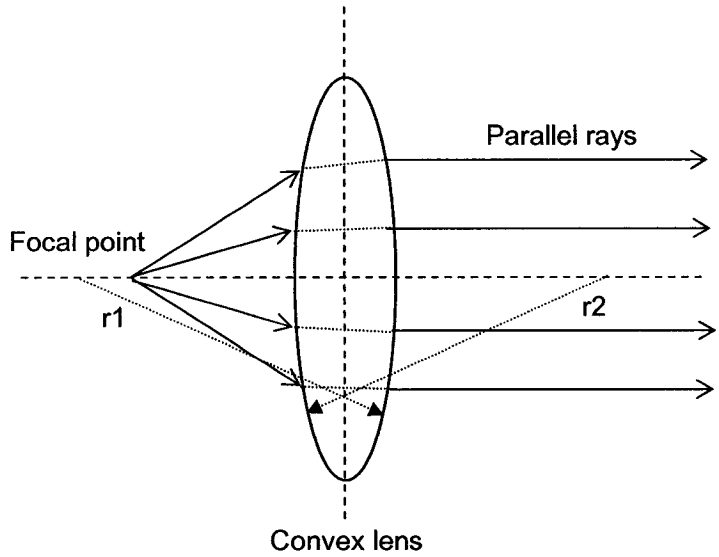

Fig. 15 Lens property

- For the relation of focus length vs lens' thickness, refer to the following figure and appendix 2.

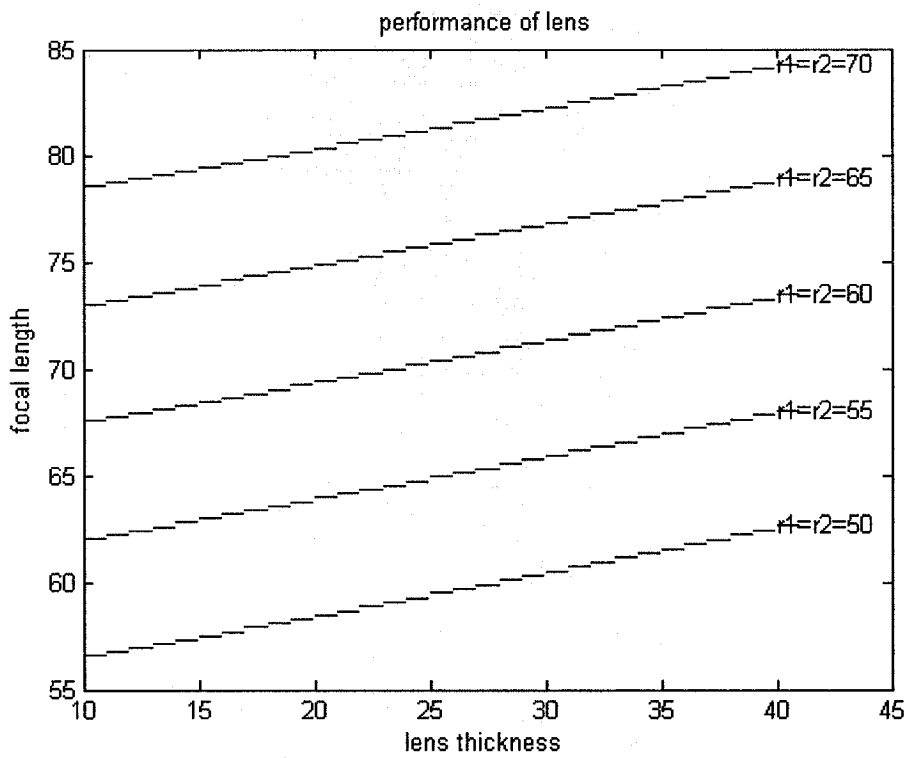

Figure 16 Relation of focus length with lens thickness

- For relation between focus length vs refractive index, refer to appendix 2

%two variables

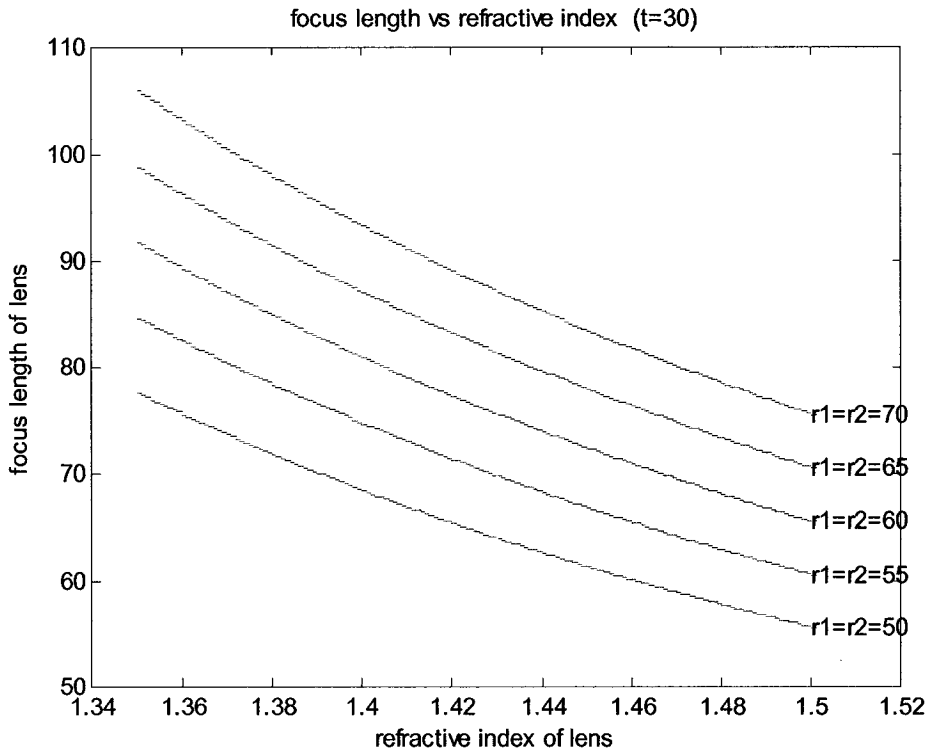

Figure 17 Relation between focus length and refractive index

Referring to the data, the parameters of lens are chosen in the design as follows:

The radius of the front and back spherical surfaces are 50μm, and the thickness of the lens is 30 μm, then the focus length is 60.5μm, this is the distance between the V-groove to the lens.

As the ratio of output to input of power loss of lens varies from 0.84 to 0.87 with the lens radius r ranging from 40um to 160um, while the thickness of the lenses t are 0. In order to get more compact structure, we set lens radius at 50μm radius. Therefore, the dimension of the lens chosen are r = 50 μm and t=30μm

For a lens of r=50 and t=30, its focal length is 60.5

Prism

The prism disperses light with various wavelengths. In order to catch the desired light with specific wavelength, we need to know the ray path. Passing through the prism, the direction of the incident rays will deviate from the original one.

- Following figure shows the relation between the incident angle and the deviation angle. Refer to appendix 3 for the calculation.

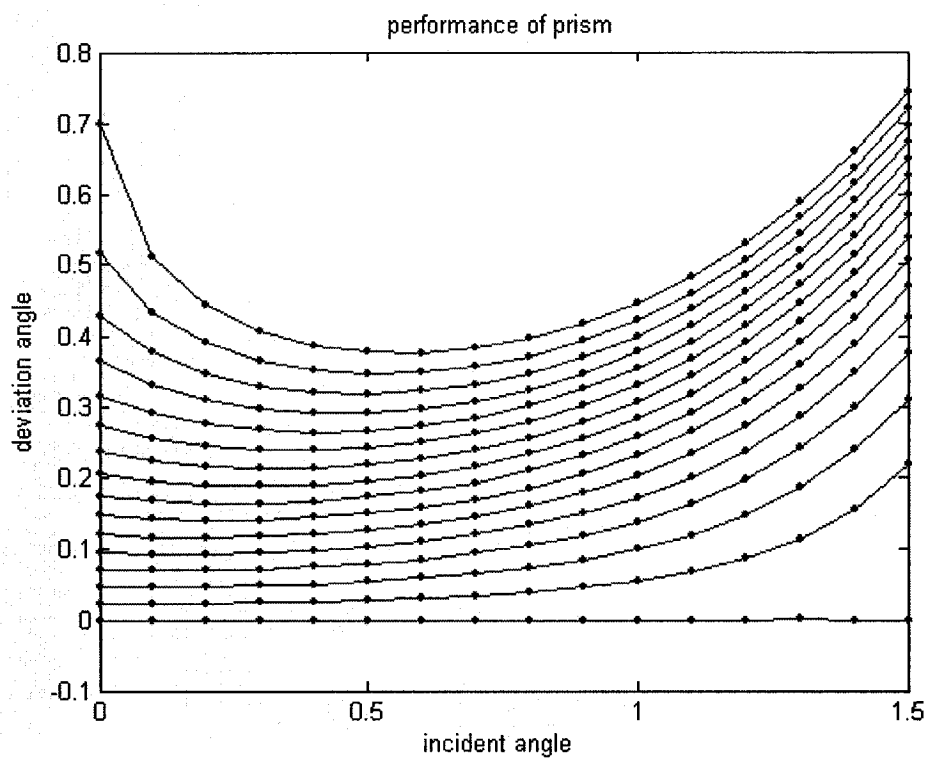

Figure 18 Relation between deviation angle and incident angle

- The calculation of the minimum deviation angle

The deviation angle will be given by the equation

$$\sin\frac{\theta+\alpha}{2} = n\sin\frac{\alpha}{2} \qquad 24$$

From the result of measurement, refractive index of SiO_2 layer n=1.377

The apex angle is set at 30 deg

Then the minimum deviation angle would be 11.76 deg

According to the discussion previously, when the refractive index at wavelength of 6250Å is1.3776, the corresponding minimum deviation angle is 11.78; when the refractive index at wavelength of 7400Å is1.370, the corresponding minimum deviation angle is 11.54, therefore, the difference of the minimum deviation angle of light at wavelength 6250Å from that of 7400Å is 11.78-11.54=0.24

If I=the incident angle, α=the apex angle, θ=the minimum deviation angle, on the condition of the minimum deviation, there exist the relation below,

$$I=(\alpha+\theta)/2$$

Therefore, the incident angle can be got as

$$I=(11.76+30)/2= 20.88$$

- The equation of the dispersed ray of light

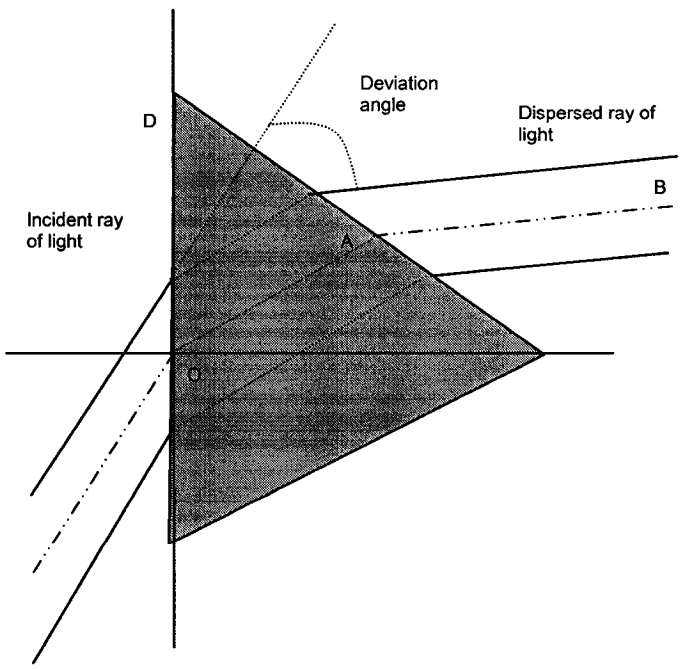

Figure 19 Light path change when light passes a prism

Assume the intersecting point of the axis of incident light with the surface of the prism is O which is used as the origin and in the middle point of the edge, the apex angle of the prism is 30 deg, the length of OD=d, then the coordinates of point A should be (OA * cos15, OA * sin15), OA=2d * cos(30/2) then the angle between line AB and x-coordinate is:

Incident angle – deviation angle=20.88-11.76=9.12 deg.

Therefore, we may determine the equation of line AB which will be used for ray-tracing for the dispersed light, that is

y- OA* sin25 =[tan(9.12)] (x-OA* cos25)

This equation gives the path of the refracted light on which the waveguide for receiving the output light will be set.

Concerning the selection of prism, there are two elements needed to be considered. One is the power loss, and the other is the apex angle. According to the simulation results of prism, the ratio of output power to input power inflates near 0.4 with apex angle varying from 15 deg. to 45deg.

Thinking about these two elements together, we will choose a prism with apex angle of 30 deg.

If apex angle is set at 30 deg., according to its relationship with the incident angle at minimum deviation, the incident angle of the light is 20.88 deg.

Mirror

The edge of planar SiO_2 layer can be used as a mirror to reflect the incident light to somewhere. Here we use it to lead the incoming light to the waveguide which is for receiving the output light. In the meantime, this mirror can separate two light rays

with adjacent wavelength much wider, then reflect the specific one to reach the specific waveguide.

Referring to the following diagram, suppose B is the position of light source, and light travel from B to A which is a point on the surface of mirror with radius r, center at the original O. The normal at point A is OO' and the angle between the normal and the incident light is α. According to Law of reflection, the light will be reflect in the direction of AC, which also has an angle α with respect to the normal at point A. Suppose the angle between OO' and OB is δ.

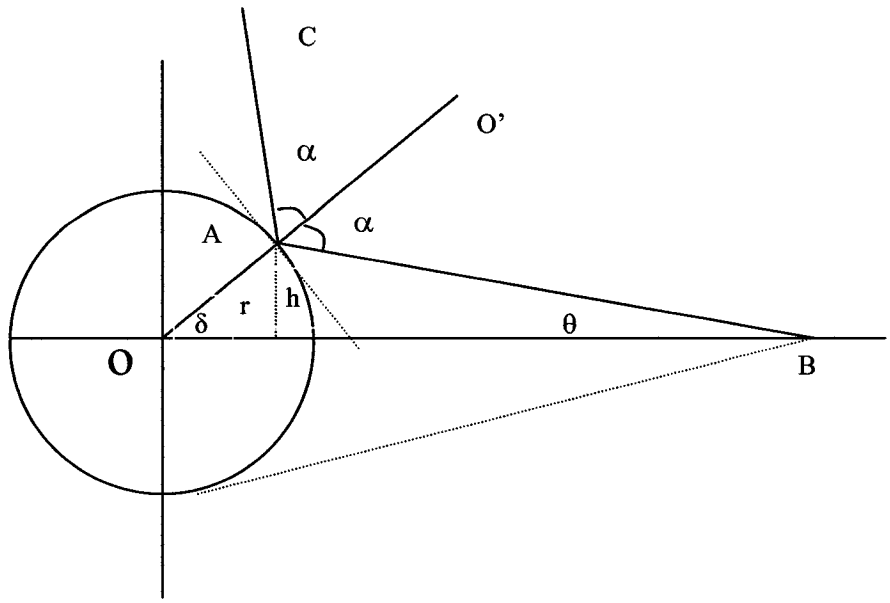

Figure 20 Reflected ray path when light encounter a mirror.

- The equation for reflected light

If the coordinate of point A is (u,v)

To get the coordinate of the point A, we need to solve the following two equations

$$x^2 + y^2 = r^2$$

$$y - 0 = (x - a)\tan(180^0 - \theta)$$

Then we get x_1 and x_2 from

$$x = \frac{2a\tan^2\theta \pm \sqrt{4a^2\tan^4\theta - 4(1+\tan^2\theta)(a^2\tan^2\theta - r^2)}}{2(1+\tan^2\theta)}$$

Then we determine the coordinate on x axis of point A by choosing the smaller value from $a-x_1$ and $a-x_2$.

Assuming x1 is what we need, so $u = x_1$

Then we get y value of point A: $v = y_1$

The slope of line AC is $k = \tan(2\delta+\theta)$

Then the equation should be

$$y-v = (x-u)\tan(2\delta+\theta)$$

This is the path which the reflected light will pass through.

Calculation of the angle θ to the spherical mirror

θ is a very important parameter in the design. Its suitable value may enable the light with needed wavelength to reach the designated position while expel unwanted wavelength from entering the waveguide.

As the figure above shows, we let OB=a

$\alpha=\theta+\delta$ if we let $\alpha=u$ $\theta=v$ $\delta=w$

then $u=v+w$

$du/dv=1+dw/dv$

also we may see

$\sin w=h/r$

$\text{ctan}v=(a-r\cos w)/h$

from these two eqation, we got

tanv=rsinw/(a-rcosw)

v=arctan[rsinw/(a-rcosw)]

then

$$dv/dw = \frac{1}{1+(\frac{r\sin w}{a-r\cos w})^2}.\frac{(a-r\cos w)r\cos w - r\sin w * r\sin w}{(a-r\cos w)^2}$$

$$= \frac{ar\cos w - r^2}{a^2 - 2ar\cos w + r^2}$$

so

$$du/dv=1+dw/dv=1+1/(\frac{ar\cos w - r^2}{a^2 - 2ar\cos w + r^2})=\frac{a^2 - ar\cos w}{ar\cos w - r^2}=d\alpha/d\theta$$

where the maximum value of w is arccos(r/a), means 0<w< arcos(r/a)

Refer to following figure and appendix 4

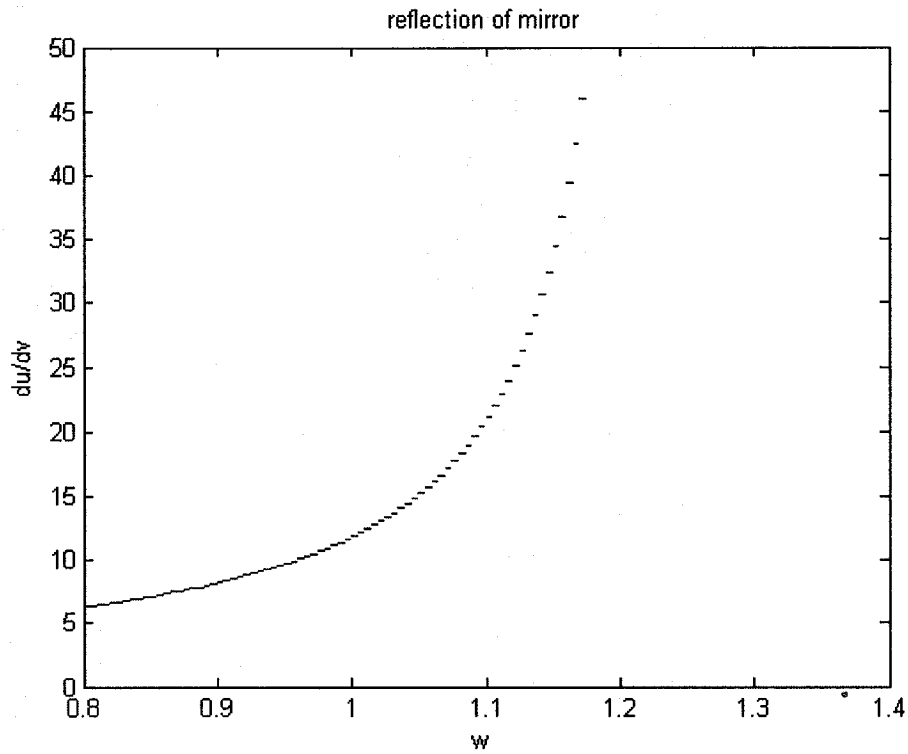

Figure 21 Reflection performance of the mirror

In order to capture the respective colors, all the wavelengths in a specified color band should go to the same receiving component. For example, the minimum wavelength of blue is 435nm and the maximum wavelength of blue is 500nm. By ray tracing these two wavelengths, we may confine the angle in which the dispersed light goes to the mirror. Refer to the following figure, the width of the waveguide which is used to receive blue light is confined 5μm which is available by the VLSI process, the distance between the mirror and the waveguide is 20μm. For approximation, we regard the two points of reflection on the surface of mirror as one point, then

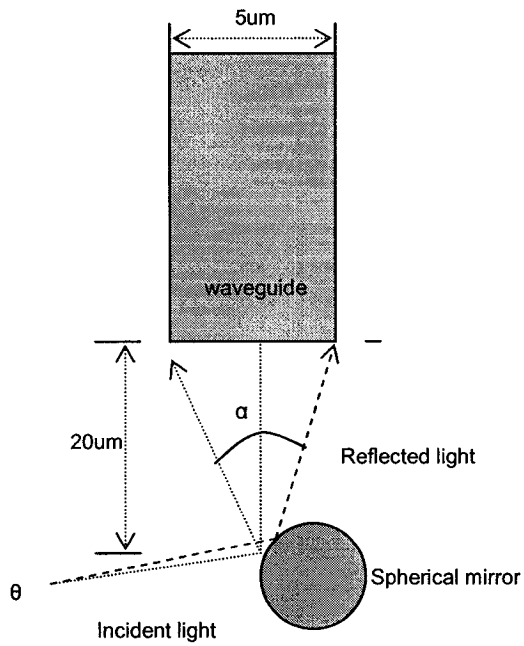

Figure 22 Reflected angle change with respect to the incident angle change

so $\alpha = 2\arctan(2.5/20)=14.25$

Concerning θ, for red color wavelength band it is 0.24

Therefore, for red color wavelength band, $d\alpha/d\theta=14.25/0.24= 59.38$

Calculated by Matlab, we may get the value of δ and θ, referring to Fig.5.1.4-1, as shown in the following table.

$d\alpha/d\theta=14.25/0.24= 59.38$

From $du/dv=1+dw/dv=1+1/(\frac{ar\cos w - r^2}{a^2 - 2ar\cos w + r^2})=\frac{a^2 - ar\cos w}{ar\cos w - r^2}=d\alpha/d\theta$

Then $\delta=w=67.82$ deg

From $\tan v=r\sin w/(a-r\cos w)$

Then

θ= v=19.45deg

The function of mirror is to reflect the separated light to a specific waveguide. In this device, we choose a spherical mirror which is able to further separate the incident lights. Only after the second time separation, the specific light can be practically coupled into the specific waveguide.

V-groove parameters

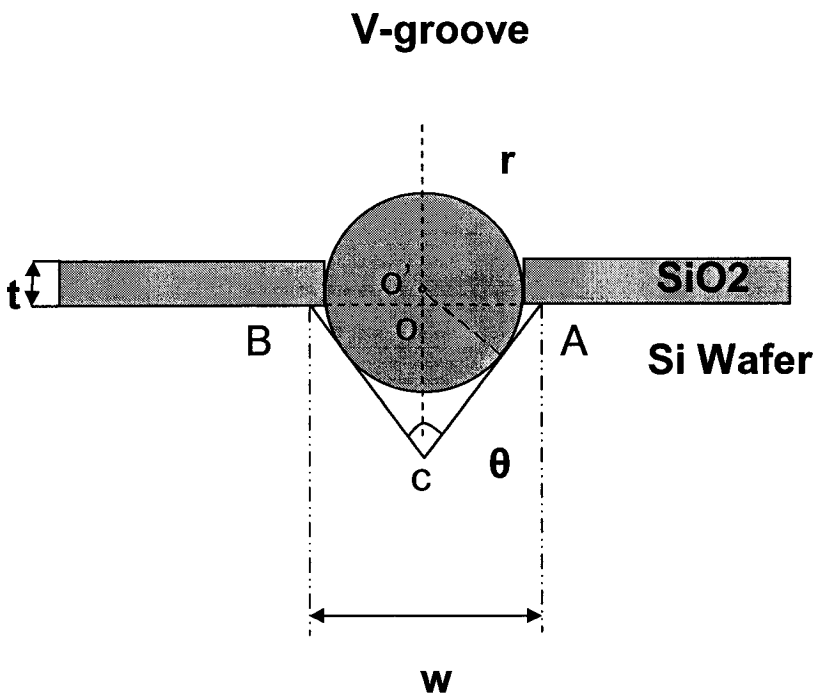

Figure 23 Side view of V-groove

The radius of fibre r=62.5μm, the thickness of the SiO2 layer is t=15μm, the center of the core of fibre is 7.5μm high above the Si wafer surface. The angle of V-groove θ on <100> Si wafer is 54.74 deg.(between the <100> and <111> crystallographic directions of silicon

o'c=r/sin(54.74/2)=135.9,

oc=o'c-7.5=128.45

oA=oc*tan(54.74/2)=66.5

AB=2*oA=133μm

This is the value of width of V-groove which is also the width of windows opened on the layout of mask

Structure of the device

The whole device is constructed by the components described below.

and the top view of the system is shown as below

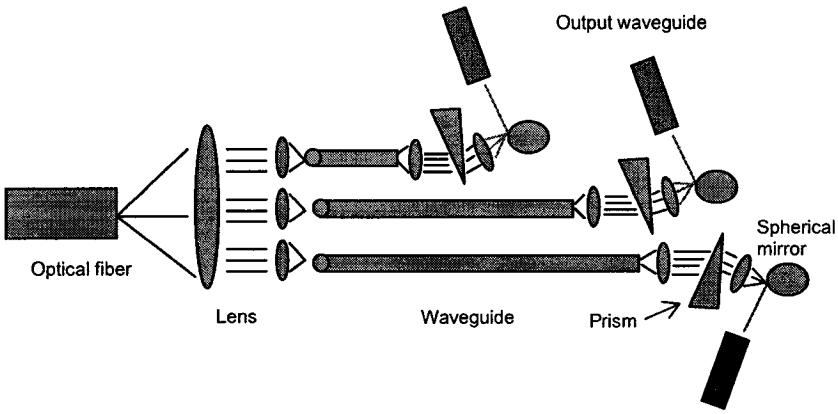

Figure 24 the structure of the device for color recognition

First, the input light signal comes along the optical fibre which is fixed at the V-groove on the surface of the substrate. Next, the lens collimates the input light into parallel light in order that three smaller lenses may receive same signals. Then, the signals are coupled into waveguides and are transmitted to the other end of the waveguide, and are sent to the prisms for diffraction. After diffraction, the particular lights with wavelength corresponding to red, blue, and green light are reflected to their particular waveguide by spherical mirrors.

The positions of all the components are calculated and all of the components are aligned at the layout level so that the system will fulfil the ray tracing requirement very well.

Wire grid polarizer

Considering the unpolarized light wave with oscillation in random directions, any of its components are able to be regarded as the superposition of two components at x-axis and y-axis, therefore, the light wave can be regarded as total superposition of those two components.

Suppose the unpolarized light is incident to a wire grid polarizer, let's say Ey components is parallel to the wire grid, Ex component is perpendicular to the wire grid,

The transmittance of the wire gird polarizer with respect to the two components comply with the following equations,

$$T_x = \frac{4nA^2}{1+(1+n)^2 A^2}$$

And $$T_y = \frac{4nB^2}{1+(1+n)^2 B^2}$$

Where n is the refractive index of (transparent) substrate material

T_x is the transmittance for component of light perpendicular to grid wires

T_y is the transmittance for component of light parallel to grid wires

$$A = \lambda/4d\left\{\ln\left[\csc\frac{\pi(d-a)}{2d}\right]+\frac{Q_2\cos^4\left[\pi(d-a)/2d\right]}{1+Q_2\sin^4\left[\pi(d-a)/2d\right]}+\frac{d^2}{16\lambda^2}\left[1-3\sin^2\frac{\pi(d-a)}{2d}\right]^2\cos^4\frac{\pi(d-a)}{2d}\right\}^{-1}$$

$$B = d/\lambda\left[\ln(\csc\frac{\pi a}{2d}) + \frac{Q_2\cos^4(\pi a/2d)}{1+Q_2\sin^4(\pi a/2d))} + \frac{d^2}{16\lambda^2}(1-3\sin^2\frac{\pi a}{2d})^2\cos^4\frac{\pi a}{2d}\right]$$

Where

$$Q_2 = \frac{1}{\left[1-(d/\lambda)^2\right]^{1/2}} - 1$$

These relations hold for grids made of metal strips of width a and spacing d when $\lambda > 2d$

From the above formulae, we may see that the distance between the wire grid should be smaller than wavelength. The smaller the distance is, the wider WGP may operate. Checking the MUMPs design rule, the allowed smallest dimension of the wire width is 2 micron, and smallest distance between two neighbour wires is also 2 micron, in this case, we choose a=2 um and d=4 um for the fabricated WGP, therefore, the wire grid polarizer may work at the far infrared region where the wavelength is longer than 10 micron.

Using Matlab programming, we may get the following figures.

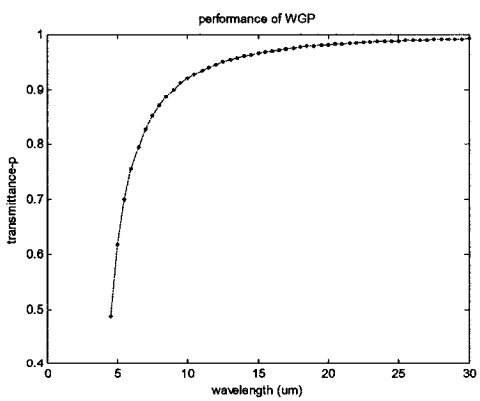

This figure shows that the component of light which is perpendicular to the wire gird will pass the grid increasingly with the increasing of wavelength.

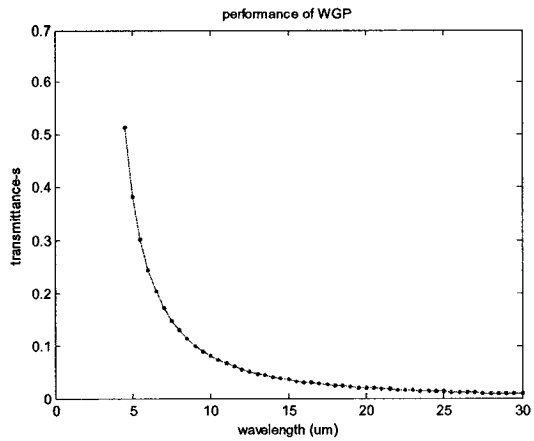

This figure shows, passing through the WGP, that the amount of the component of light which is parallel to the wire gird will decrease rapidly with the increasing of wavelength.

These figures theoretically proved that, with regard to the fabricated WGP, the the longer the wavelength of light is, the much polarization will happen when the light pass through wire grid polarizer. As shown in the figure, at wavelength of 20μm, T_x ≈98%, $T_y \approx 2\%$.

Different from current wire grid polarizer which uses aluminium to make polarizer, we make use of polysilicon as material to fabricate the device. This polysilicon called poly 2 is one of the 3 polysilicon layers which are separated by SiO_2 material. As a sacrifice layer, SiO_2 will be etched away in the final fabrication process. The thickness of the polysilicon for WGP is 2 μm. As the polysilicon is deposited on a substrate, after WGP is fabricated, it needs to be flipped up. In this case, two holders with lock structures are designed to support the polarizer. These two holders are fabricated on the poly1 layer. In order to flip up the holders and polarizer freely, several micro hinges structures are fabricated making use of poly 1 and poly 0.

The device has three parts. Refer to the following picture of the device.

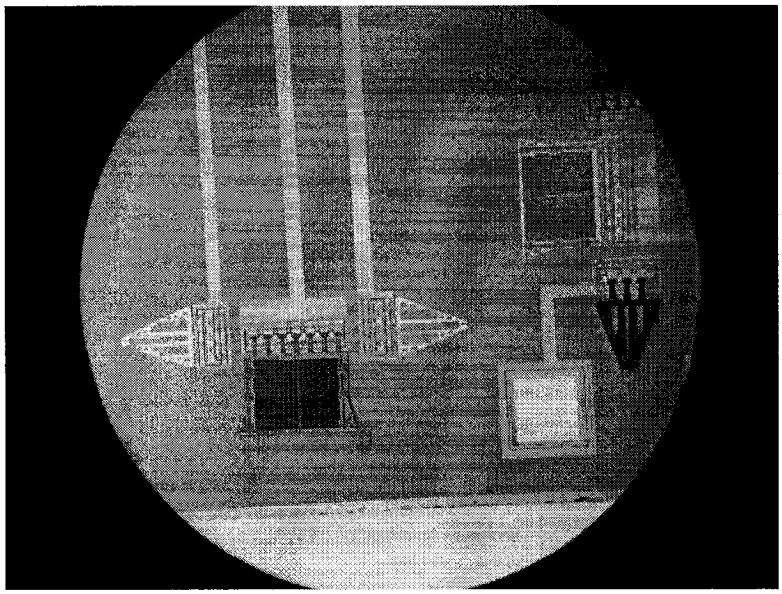

Fig. 25 Wire grid polarizer made by MUMPs process

As picture show, two triangular parts are holders. The rectangular part is polarizer. Each part has its own pad enabling it to connect with electric circuits separately. These 3 parts flip up and two holders may stabilize the polarizer.

Section 3.2 Fabrication of Micro optical components

In this project, some separated components like lens, prisms, and waveguides are fabricated. In the meantime, as an application of these components, a device for color recognition purpose is also fabricated at the same time. Totally different from the traditional optical component process, this optical device makes use of VLSI process to integrate many optical components at one time on the Si wafer, and these components do not need to be mounted on the precise frames, aligned carefully among each other after fabrication.

Lithography

Lithography enable the designed pattern "printed" by radiation on the mask like photoresists on the surface of substrate. During lithography, the exposing

radiation pass through the "clear" parts of a mask, whereas the designed pattern of opaque chromium prevent some of the radiation from passing.

There are several kinds of radiation sources with different wavelength of light. For example, ultraviolet (UV) light, electrons exposing, x-rays exposing, or ions exposing. In this project, UV light is applied.

Photo-resists are of two types. A negative resist on exposure to light becomes less soluble in a developer solution, while a positive resist becomes more soluble. For negative resists, the developer solvent dissolves the unexposed resist. For positive resists, the developer solvent dissolves the exposed resist. Comparatively, higher resolution is possible with positive resists. And this is the option for this project.

In terms of the distance between mask and substrate, shadow (proximity) printing may be employed where the gap between mask and wafer is small. In the case of a nonexistent gap, the method is called contact printing. In order to get high resolution, we chose contact printing.

According to the process designed, several masks are needed to fabricate the device. Every mask contains the specifications like length, width, and depth, as well as the layout of the components of as lens, mirror, prisms, and waveguides. At different processing step, the mask needed is different.

Once the masks are made, the resist material is spin-coated onto the wafer. Then the resist on the wafer is exposed to a sensitizing source through the mask so that the mask pattern is transferred onto the resist. Here, positive photoresist is applied.

The sensitized resist is then developed in a solvent so that the desired pattern emerges after the development for the actual device fabrication steps such as film deposition, plasma etching, etc, that are specified by the mask and masking level. In

essence, repetition of lithographic processing constitutes the entire device fabrication procedure. Each time the cycle is repeated, the new mask pattern has to be aligned to the pattern already present on the wafer.

In this design, there are 2 masks needed for V-groove and optical components, respectively.

Oxidation

Silicon dioxide layer on the surface of Si wafer serves as the layer on which the optical components will be made in this design. The oxidation mechanism is that, because a silicon surface has a high affinity for oxygen, an oxide layer rapidly forms when silicon is exposed to an oxidizing ambient.

The equation below is used to calculate the thickness of the SiO_2 layer when time, temperature, and ambient of the process are given

$$\frac{d_0}{A/2} = [1 + \frac{t+\tau}{A^2/4B}]^{1/2} - 1$$

Where d_0 is the oxide thickness, A and B are two rate constants which are orientation dependent and may be checked out from the tables. τ represents a shift in the time coordinate to account for the presence of the initial oxide layer d_i, t is the oxidation time.

One limiting case occurs for long oxidation times when $t>>\tau$ and $t>>A^2/4B$.

$$d_0^2 = Bt$$

The other limiting case occurs for short times when $(t+\tau) << A^2/4B$.

$$d_0 = \frac{B}{A}(t+\tau)$$

In this device, the thickness of the SiO_2 layer should be 10μm or more in order to have a satisfied coupling of input and output lights.

The stress associated with the SiO_2 layer should be paid attention. During device processing, windows are cut into the oxide, resulting in a complex stress distribution. Exceedingly high stress levels can occur at these discontinuities. All these stress levels can contribute to film cracking. The stress will be one cause for the increasing of light power loss.

Etching

There are several types of etching techniques. In terms of etching direction, there are isotropical and anisotropical etchings. If the etching process attacks the layer surface equally in all directions, the etching is said to be isotropic. Most liquid etches are isotropic and result in the undercut of the mask and the narrowing of the feature. If the etching process attacks the layer significantly faster in the vertical direction than in the horizontal, the etching is said to be anisotropic. For example - HF: water solution is etching SiO_2 very rapidly in all direction while not etching silicon. Whereas. Plasma etching is applied to anisotropic etching not only for Si but also for SiO_2.

In order to couple lights among components and fibre optics, the edge of components like lens, prism, and mirrors should be etched as perpendicular to the surface of the substrate as possible. Therefore plasma etching process is applied.

Silicon micromachining techniques

The main silicon micromachining techniques can be divided into two groups: bulk and surface micromachining. Bulk micromachining usually refers to etching through the wafer form the back side to form the desired structures.

The designed structures are generally got by making use of wet anisotropic etchants. These etchants have the important property of an etch rate that is dependent upon crystal orientation. Just because of the different etch rate of the different planes, we may get specific geometric structure called V-groove on the silicon surface which may be used as bonding structure for fibre optics.

The main etchants used are ethylenediamine and pyrocatechol(EDP), potassium hydroxide(KOH), and tetramethyl ammonium hydroxide(TMAH), etc.

V-grooves is wet etched in <100> oriented silicon substrate. Commonly used anisotropic etchants are solutions of KOH or EDP that permit the V to be made with an angle of 54.74 deg between the <100> and <111> crystallographic directions of silicon. The use of a silicon V-groove permits one to precisely control the desired groove shape and to ensure that the vertical positions of the cores of fibre placed in the V-groove are aligned with optical components like lens and waveguide.

MUMPs process for wire grid polarizer

The MUMPs process is a three-layer polysilicon surface micromachining process derived from work performed at the Berkeley Sensors and Actuators Center (BSAC) at the University of California.

The process begins with 100 mm n-type (100) silicon wafers of 1-2 ohm-cm resistance. The surfaces of the wafers are first heavily doped with phosphorus in a standard diffusion furnace using $POCl_3$ as the dopant source. Next, a 600 nm low-stress LPCVD (low pressure chemical vapor deposition) silicon nitride layer is deposited on the wafers. This is followed directly by the deposition of a 500 nm LPCVD polysilicon film-Poly 0. Poly 0 is then patterned by photolithography, a process that includes the coating of the wafers with photoresist (Figure 26), exposure

of the photoresist with the appropriate mask and developing the exposed photoresist to create the desired etch mask for subsequent pattern transfer into the underlying layer (Figure 27). After patterning the photoresist, the Poly 0 layer is then etched in an RIE (Reactive Ion Etch) system (Figure 28). A 2.0 μm phosphosilicate glass (PSG) sacrificial layer is then deposited by LPCVD (Figure 29). The sacrificial layer is lithographically patterned with the DIMPLES mask and the dimples are transferred into the sacrificial PSG layer by RIE, as shown in Figure 30. The wafers are then patterned with the third mask layer, ANCHOR1, and reactive ion etched (Figure 31).

After etching ANCHOR1, the first structural layer of polysilicon (Poly 1) is deposited at a thickness of 2.0 μm. A thin (200 nm) layer of PSG is deposited over the polysilicon and the wafer is annealed at 1050°C for 1 hour (Figure 32). The anneal dopes the polysilicon with phosphorus from the PSG layers both above and below it. Besides, the anneal also serves to significantly reduce the net stress in the Poly 1 layer. The polysilicon (and its PSG masking layer) is lithographically patterned using a mask designed to form the first structural layer POLY1. The PSG layer is etched to produce a hard mask for the subsequent polysilicon etch. After etching the polysilicon (Figure 33), the photoresist is stripped and the remaining oxide hard mask is removed by RIE.

After Poly 1 is etched, a second PSG layer (Second Oxide) is deposited (Figure 34). The Second Oxide is patterned using two different etch masks with different objectives. The POLY1_POLY2_VIA layer is lithographically patterned and etched by RIE (Figure 35). The ANCHOR2 level is provided to etch both the First and Second Oxide layers in one step, thereby eliminating any mis-alignment between separately etched holes. More importantly, the ANCHOR2 etch eliminates the need to make a cut in First Oxide unrelated to anchoring a Poly 1 structure, which needlessly

exposes the substrate to subsequent processing that can damage either Poly 0 or nitride. The ANCHOR2 layer is lithographically patterned and etched by RIE in the same way as POLY1_POLY2_VIA. Figure 36 shows the wafer cross section after both POLY1_POLY2_VIA and ANCHOR2 levels have been completed. The second structural layer, Poly 2, is then deposited (1.5 μm thick) followed by the deposition of 200 nm PSG. As with Poly 1, the thin PSG layer acts as both an etch mask and dopant source for Poly 2 (Figure 37). The wafer is annealed for one hour at 1050° C to dope the polysilicon and reduce the residual film stress. The Poly 2 layer is lithographically patterned with the seventh mask (POLY2) and the PSG and polysilicon layers are etched by RIE using the same processing conditions as for Poly 1. The photoresist then is stripped and the masking oxide is removed (Figure 38).

The final deposited layer in the MUMPs process is a 0.5 μm metal layer that provides for probing, bonding, electrical routing and highly reflective mirror surfaces. The wafer is patterned lithographically with the eighth mask (METAL) and the metal is deposited and patterned using lift-off. The final, unreleased structure is shown in Figure 39. The wafers are diced, sorted and shipped to the MUMPs user for sacrificial release and test. Figure 40 shows the device after sacrificial oxide release.

The release is performed by immersing the chip in a bath of 49% HF (room temperature) for 1.5-2 minutes. This is followed by several minutes in DI water and then alcohol to reduce stiction followed by at least 10 minutes in an oven at 110° C.

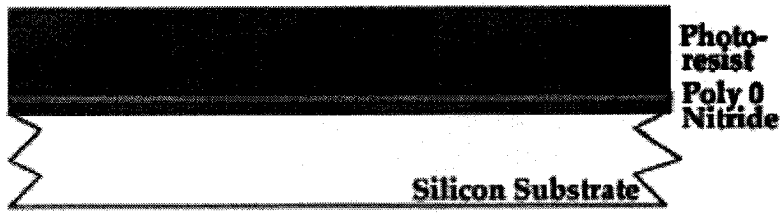

Fig.26 The surfaces of the starting n-type (100) wafers are heavily doped with phosphorus in a standard diffusion furnace using POCl3 as the dopant source. A 600 nm blanket layer of low stress silicon nitride (Nitride) is deposited followed by a

blanket layer of 500 nm polysilicon (Poly 0). The wafers are then coated with UV-sensitive photoresist.

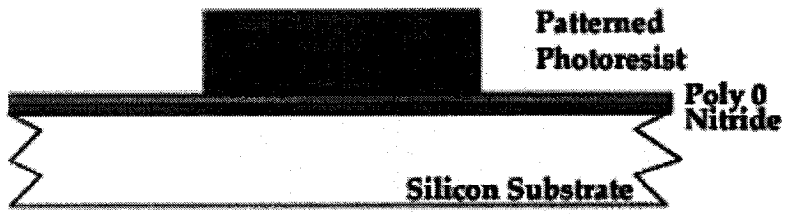

Figure 27 The photoresist is lithographically patterned by exposing it to UV light through the first level mask (POLY0) and then developing it . The photoresist in exposed areas is removed leaving behind a patterned photoresist mask for etching.

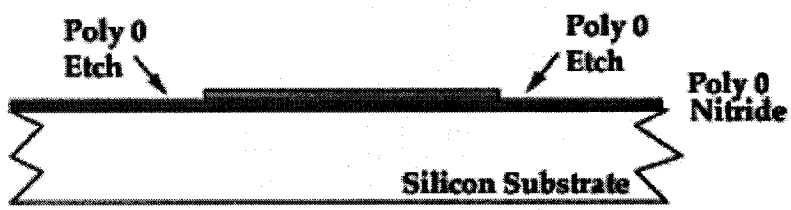

Figure 28 Reactive ion etching (RIE) is used to remove the unwanted polysilicon. After the etching, the photoresist is chemically stripped in a solvent bath. This method

of patterning the wafers with photoresist, etching and stripping the remaining photoresist is used repeatedly in the MUMPs process.

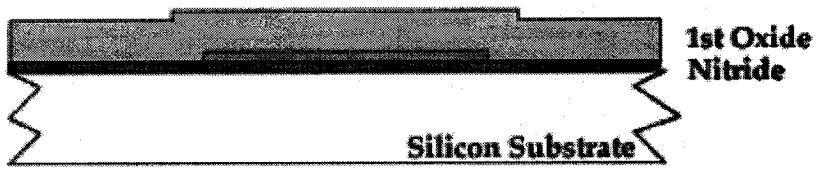

Figure 29 A 2.0 μm layer of PSG is deposited on the wafers by low pressure chemical vapor deposition (LPCVD). This is the first sacrifical layer.

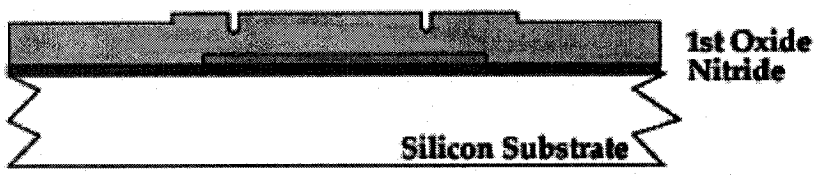

Figure 30 The wafers are coated with photoresist and the second level (DIMPLE) is lithographically patterned. The dimples, 750 nm deep, are reactive ion etched into the first oxide layer. After the etching, the photoresist is stripped.

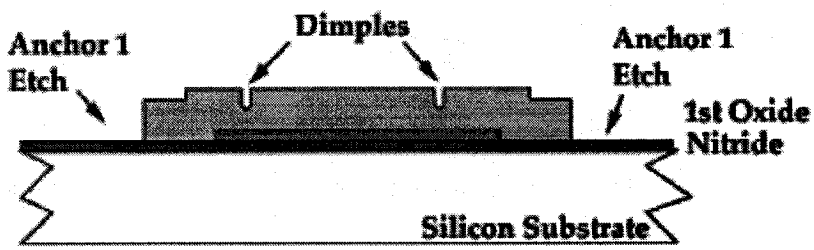

Figure 31 The wafers are re-coated with photoresist and the third level (ANCHOR1) is lithographically patterned. The unwanted oxide is removed in an RIE etch and the photoresist is stripped.

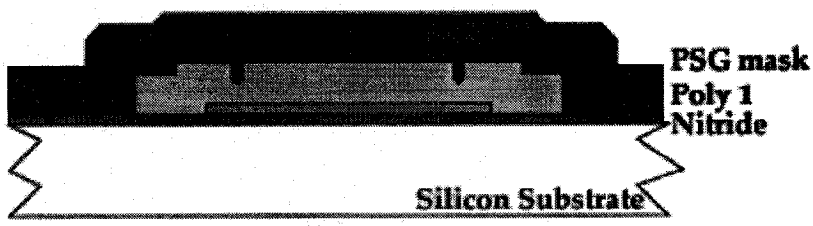

Figure 32 Blanket 2.0 μm layer of un-doped polysilicon is deposited by LPCVD followed by the deposition of 200 nm PSG and a 1050° C/1 hour anneal. The anneal serves to both dope the polysilicon and reduce its residual stress.

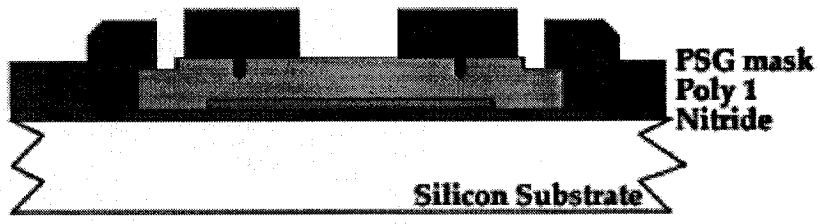

Figure 33 The wafer is coated with photoresist and the fourth level (POLY1) is lithographically patterned. The PSG is first etched to create a hard mask and then Poly 1 is etched by RIE. After the etching is completed, the photoresist and PSG hard mask are removed.

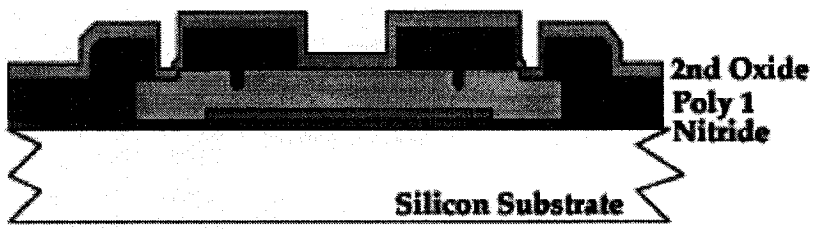

Figure 34 The Second Oxide layer, 0.75 μm of PSG, is deposited on the wafer. This layer is patterned twice to allow contact to both Poly 1 and substrate layers.

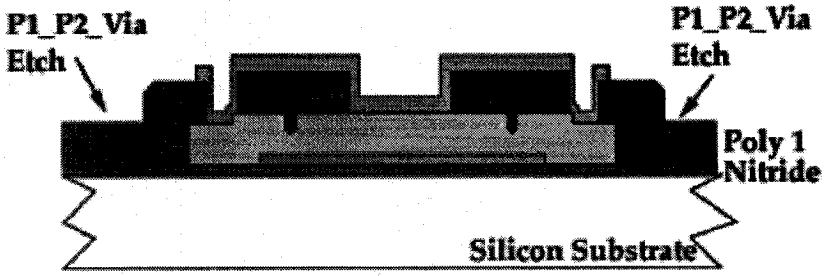

Figure 35 The wafer is coated with photoresist and the fifth level (POLY1_POLY2_VIA) is lithographically patterned. The unwanted Second Oxide is RIE etched, stopping on Poly 1, and the photoresist is stripped.

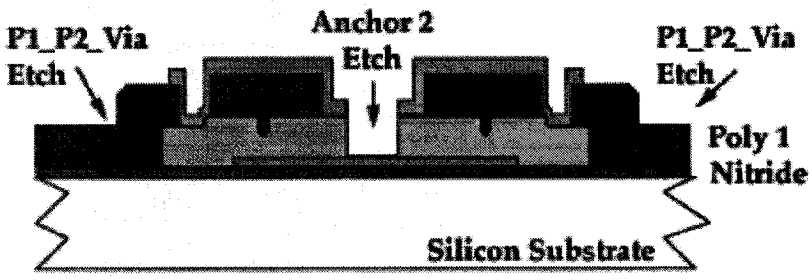

Figure 36 The wafer is re-coated with photoresist and the sixth level (ANCHOR2) is lithographically patterned. The Second and First Oxides are RIE etched, stopping on either Nitride or Poly 0, and the photoresist is stripped. The ANCHOR2 level provides openings for Poly 2 to contact with Nitride or Poly 0.

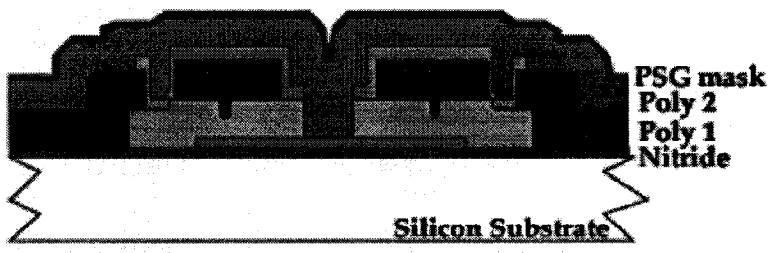

Figure 37 A 1.5 μm un-doped polysilicon layer is deposited follwed by a 200 nm PSG hardmask layer. The wafers are annealed at 1050°C for one hour to dope the polysilicon and reduce residual stress.

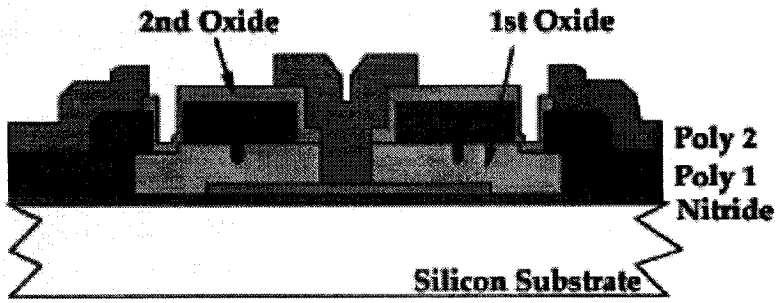

Figure 38 The wafer is coated with photoresist and the seventh level (POLY2) is lithographically patterned. The PSG hard mask and Poly 2 layers are RIE etched and the photoresist and hard mask are removed. All mechanical structures have now been fabricated. The remaining steps are to deposit the metal layer and remove the sacrificial oxides

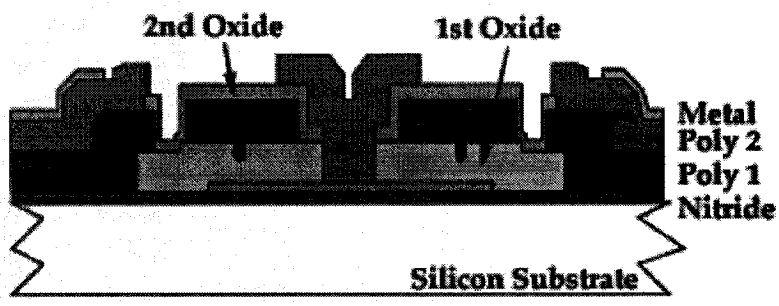

Figure 39 The wafer is coated with photoresist and the eighth level (METAL) is lithographically patterned. The metal (gold with a thin adhesion layer) is deposited by lift-off patterning which does not require etching. The side wall of the photoresist is sloped at a reentrant angle, which allows the metal to be deposited on the surfaces of the wafer and the photoresist, but provides breaks in the continuity of the metal over the reentrant photoresist step. The photoresist and unwanted metal are then removed in a solvent bath. The process is now complete and the wafers can be coated with a protective layer of photoresist and diced. The chips are sorted and shipped.

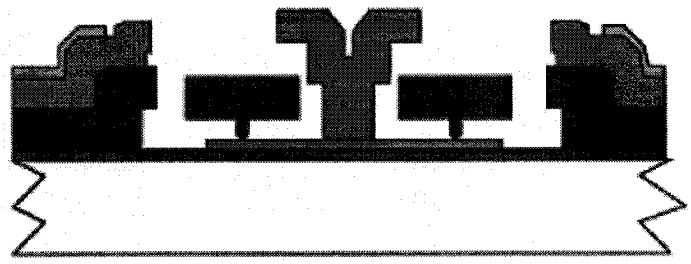

Figure 40 The structures are released by immersing the chips in a 49% HF solution. The Poly 1 ``rotor'' can be seen around the fixed Poly 2 hub. The stacks of Poly 1, Poly 2 and Metal on the sides represent the stators used to drive the motor electrostatically.

Material Layer	Thickness (μm)	Lithography Level Name
Nitride	0.6	-
Poly 0	0.5	POLY0 (HOLE0)
First Oxide	2.0	DIMPLE
		ANCHOR1
Poly 1	2.0	POLY1 (HOLE1)
Second Oxide	0.75	POLY1_POLY2_VIA
		ANCHOR2
Poly 2	1.5	POLY2 (HOLE2)
Metal	0.5	METAL (HOLEM)

Table 2 Layer names, thicknesses and lithography levels. Hole levels are printed on the same line as their corresponding polysilicon or metal levels .

Mnemonic Level Name	Field Type	Purpose
POLY0	light	pattern ground plane
ANCHOR1	dark	open holes for Poly 1 to Nitride or Poly 0 connection
DIMPLE	dark	create dimples/bushings for Poly 1
POLY1	light	pattern Poly 1
POLY1_POLY2_VIA	dark	open holes for Poly 1 to Poly 2 connection
ANCHOR2	dark	open holes for Poly 2 to Nitride or Poly 0 connection
POLY2	light	pattern Poly 2
METAL	light	pattern Metal
HOLE0	dark	provide holes for POLY0
HOLE1	dark	provide release holes for POLY1
HOLE2	dark	provide release holes for POLY2
HOLEM	dark	provide release holes in METAL

Table 3 lists the field convention used in the MCNC process and a brief description of the purpose of each level.

Process for color recognition device

1. Si wafer preparation

   In this device, we need Si wafer with Miller indices (100)

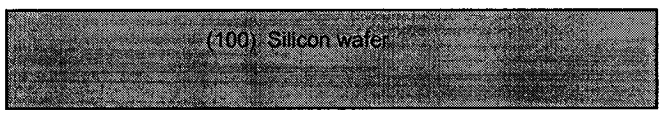

2. Wafer oxidation

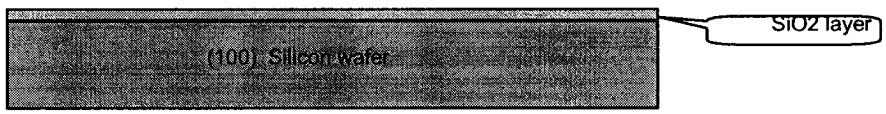

   the thickness of the SiO2 layer should be around 10um

3. Coating Al film on the surface of silica

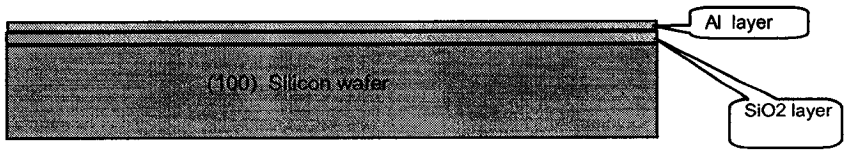

Making use of Vacuum evaporator to deposit Al film on top of SiO2

4. Coating photoresist film

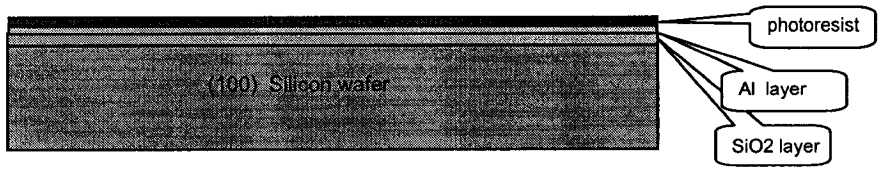

In this process, positive photoresist is applied.

5. Lithography

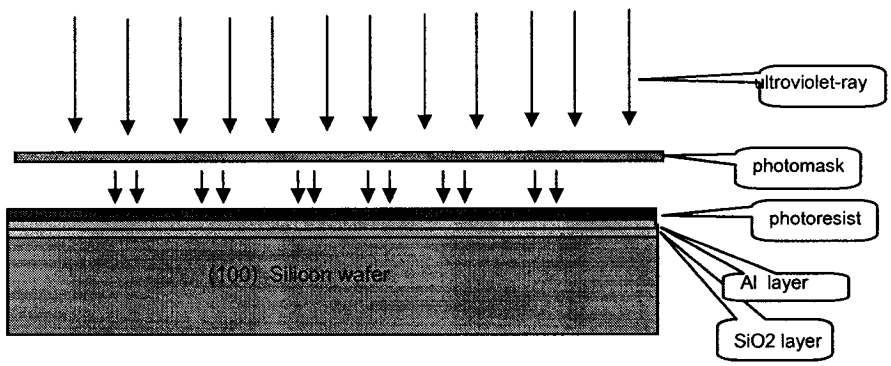

5. Development of photresist film

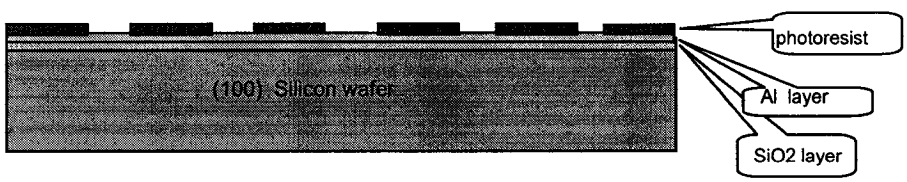

6. Plasma-etching of patterned silica to construct lens areas, waveguides areas, prism areas and mirror areas

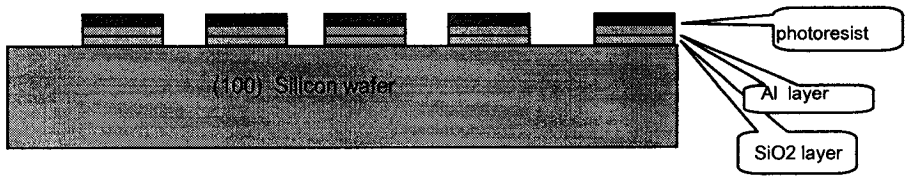

7.Coating photoresist

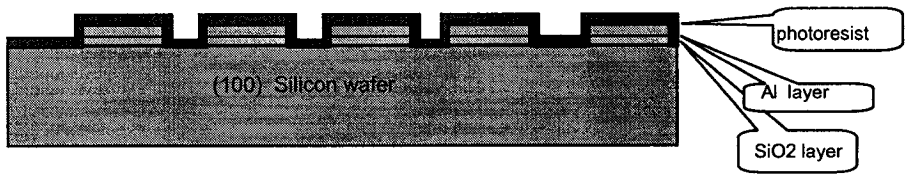

8.Patterning photoresist layer for V-groove

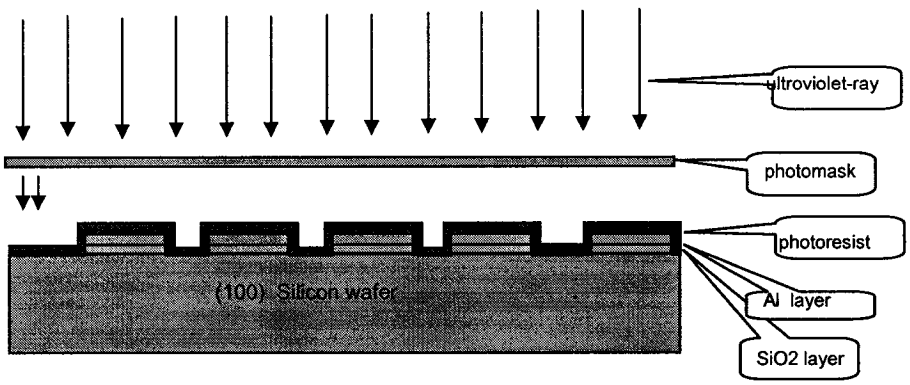

9. Developing photoresist

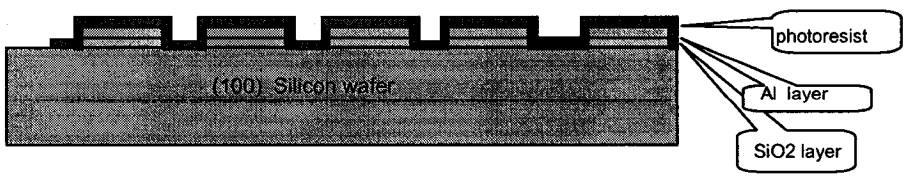

10. Etching out areas for V-groove.

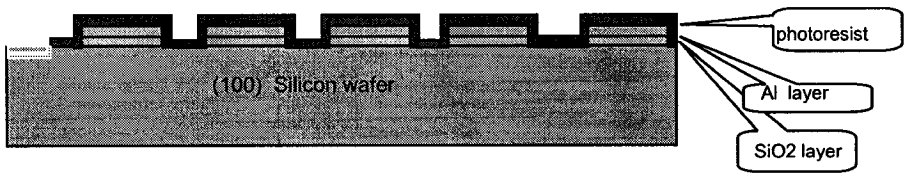

11.Removing photoresist.

(End of Chapter 3) Continue:

Chapter 4 Discussion and Conclusion

Discussion of the 2 fabricated device

Conclusion

Chapter 4 Discussion and Conclusion

- **Micro device for color recognition**

Color recognition technique has been widely used in many fields. In industry fields, it is used to do analyses of the elements of the medicine, to sort out some parts in the manufacture process, to realize production automation and image signal processing [7]. In artificial vision fields, it mimics the function of human vision to let the blind and the color-blind see the real world. It is also a tool for biomedical use, the measurement of pollutants, human burn injury, and industrial controls [8]. In domains such as road/highway scenes, off-road navigation and military target detection, the technique also plays its roles [9].

In terms of the fabrication technology, micromachining technique has been used to create miniature structure of color recognition device [10], the techniques employed borrow heavily from the microelectronics industry. Another method is to use a system based on artificial neural networks which kind of application are plentiful in industry and the community[11]; additionally, semiconductor properties and technologies are used to fabricate PIN color detectors which may determine spectral response data[7]; using led and software techniques, color recognition is also achieved [8]

At present, most of the core of the devices used for color recognition made of semiconductor materials are various kind of PIN diodes [12] [13].

The ideas of the devices in this project (Refer to Fig. 41, Fig.42, Fig. 43, and Fig.44) come from the combination of VLSI technology with micro-optical components. With the help of matured VLSI technology, it is possible to miniature

the dimensions of optical components into micron level so as to make micro optical components be compatible with optical fibre technology and optical integrated circuit.

Compared with the current optical products with the same function, the advantages of these devices are easy to make alignment, easy to change the design parameter to meet the customer requirements. No grinding needed. All the optical components are integrated on the substrate and very complicated mounting procedure and mounting parts [14] to guarantee the alignment of the optical components are unnecessary in this device. [15].

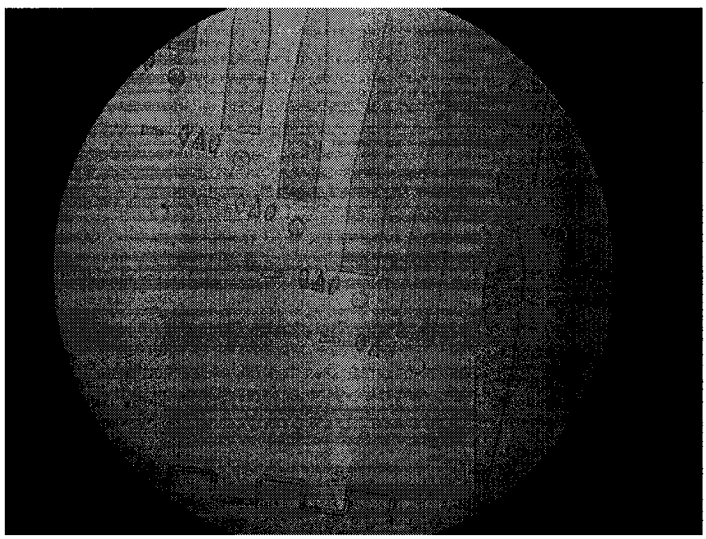

Fig. 41 Top view of the device for color recognition (Magnification10x10)

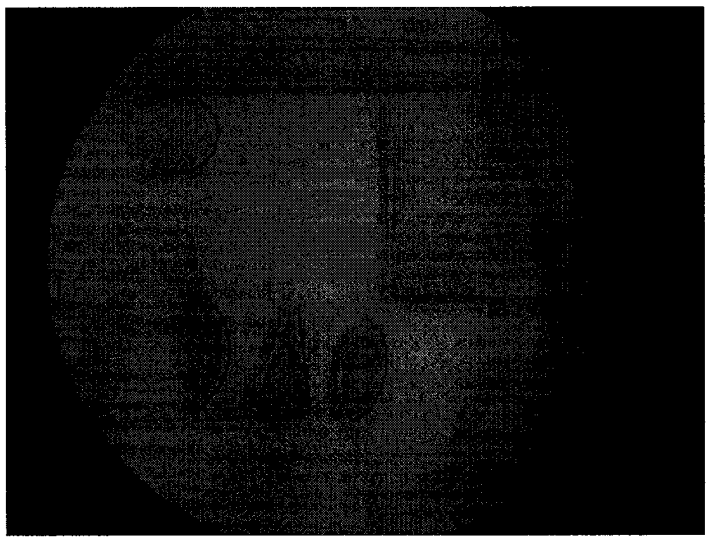

Fig 42 Top view of the device for color recognition (Magnification50x10)

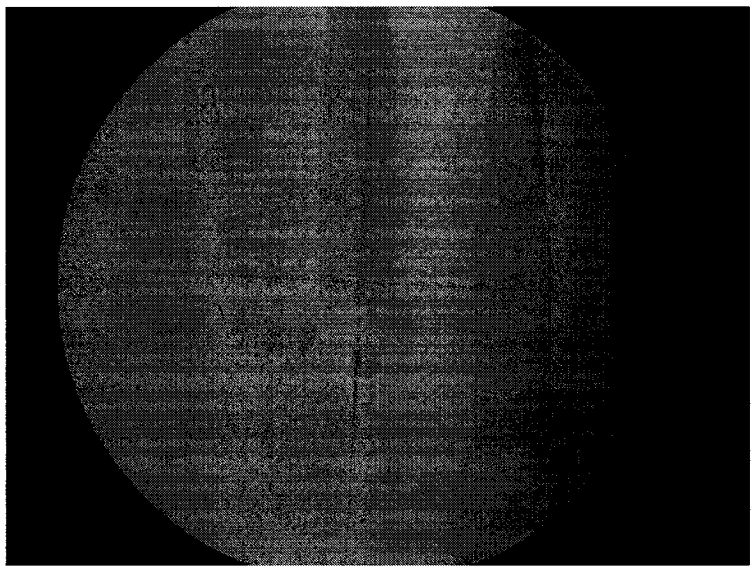

Fig.43. Top view of the device for color recognition (Magnification20x10)

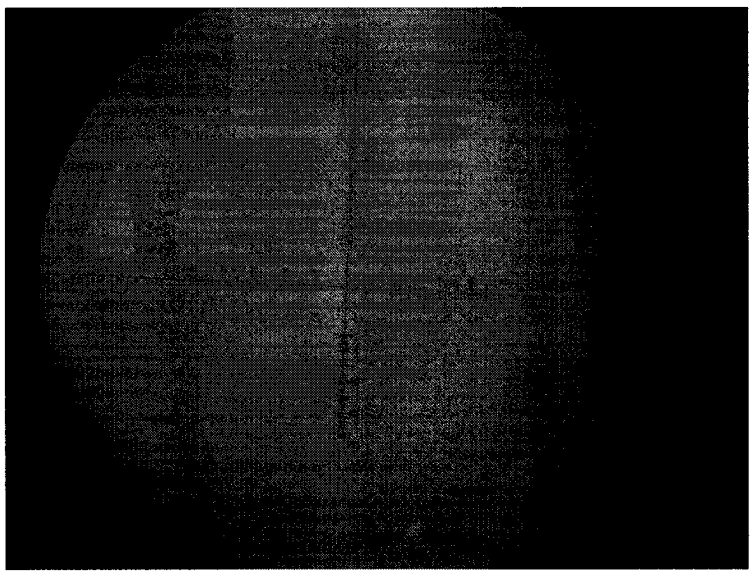

Fig.44. Top view of the device for color recognition (Magnification 50x10)

In the above pictures, the round shape components are mirrors, the triangular ones are prisms, and the long rectangular ones with sharp ends are waveguides for light transmissions.

In the device for color recognition, the width of the lens is 30μm, the front and back surface radius of the lens is 50μm; the apex angle of the prism is 30deg and the length of edges of the prism are 60μm. The width of the waveguide is from 10μm to 100μm.

It can be seen that the shape of the components is very satisfactory. Without general steps of surface grinding and polishing after optical components fabrication, the curvature of the optical components is very smooth. Moreover, the alignments after fabrication among these optical components are already preset at layout level. Compared with traditional way to make optical components, the process is simple, precise, and efficient.

- **Micro device for polarization**

WGPs have been used in the past to polarize infrared light and narrow bands for over110 years. WGP for 6um to 20um region was reported fabricated [16][17], where ion-beam sputtering and laser holographic techniques were ever used. In recent years, many companies use aluminium evaporation process and high resolution lithographic technology to get current-used WGP, their wavelength range are throughout visible spectrum [19]. Common point among these WGP is that they are at least in millimeters scales in terms of their demensions. Using MUMPs process, a micron scale WGP has been fabricated, and it is shown in Figure 45.

Compared with currently used polarizers which use metal strips, this WGP used polysilicon material to make wire strip. This created the possibility to fabricate it at the same time with other microelectronic devices which are normally fabricated on Si substrate. Other polarizers need substrate like SiO_2 to make wire grid. As a planar fabrication process, facilities currently for the fabrication of microelectronic device can be used directly.

Top view of the device

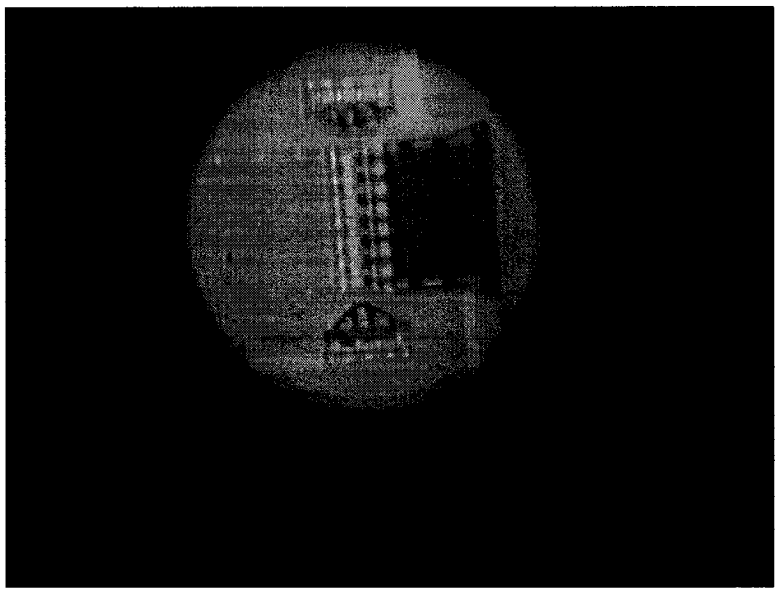

Fig 45 Two holders flipped up

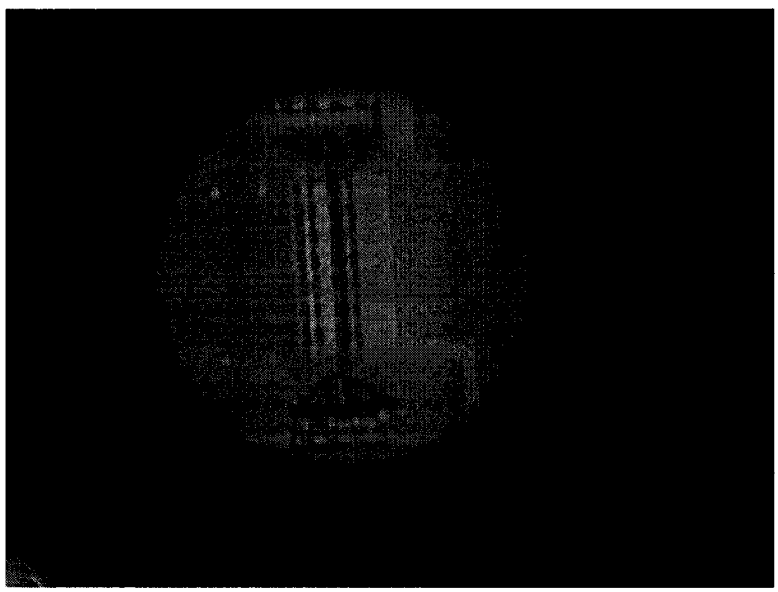

Fig. 46 Polarizer flipped up with two holders

In the pictures of micro wire grid polarizer, the yellow rectangular parts are hinges, the two triangle parts are holders with lock structure, and the rectangular part is polarizer. The yellow rectangular lines are poly wires connecting to the pads respectively.

The wire grid polarizer made by MUMPs process has wire grid width of 2 μm, the period of the grid is also 2μm, which was the smallest dimension that MUMPs process could reach when fabricated. The width and the height of polarizer are 200μm and 300μm respectively. These dimensions are large enough for light coupled from optical fiber to pass. The micro hinges may rotate at their position freely so that each part may be flipped up. By observation, several devices made on the same die had lost one holder or the polarizer when the dies were received. The reason may be because of a supercritical CO_2 process in MUMPs to ensure all the solution for releasing dry out completely, as the holders and polarizer is very tender micro parts, they perhaps can not stand improper CO_2 blowing.

Conclusion

New types of micro planar optical components (MPOC) are fabricated on Si substrate for the first time. Based on the study of these components, an optical device is designed for purpose of color recognition. The fabrication process of the micro planar optical components employed in the project is similar to VLSI process. According to the theory of Physics Optics and software simulation, power loss rate of micro planar optical components are discussed and determined. With the help of Matlab software programming, Geometric Optics is applied to calculate light path in order that light can be controlled to travel in specific route. As the specific cases for applying the micro planar optical components, a micro planar optical device for color recognition is designed and fabricated in our lab.

Micro wire grid polarizer is designed and fabricated using MUMP technologies with the support of Canadian Microelectronic Corporation (CMC). The smallest dimension in the design rules can be well reached to realize the design

purposes. The design rules and the MUMPs process are very practical for the fabrication of WGP.

The processes for the fabrication are very cost-effective solutions and new methods for making micro optical components and may be available to deliver complex optical integrated circuits that offer increased scalability and superior performance to satisfy future demands in terms of performance, cost and manufacturability.

References

1. S.S.Akhmanov and S.Yu. Nikitin, "Physical Optics", Department of Physics, M.V. Lomonosov Moscow State University. Claredon press, Oxford, 1997
2. Robert O. Naess, "Optics for Technology Students", Retired Professor of Electromechanical Technologies, Rochester Institute of Technology, Rochester, New York, Prentice Hall, 2001
3. http://www.semiconfareast.com/polysilicon.htm
4. Donald C. O'shea, "Elements of Modern Optical Design", School of Physics, Georgia Institute of Technology, Atlanta, Georgia, 1985
5. J.F.James and R.S.Sternberg, "The design of Optical Spectrometers", Lectures in Physics in the University of Manchester, 1969
6. Gerd Keiser, "Optical Fiber Communications", Third Edition, GTE Systems and Technology Corporation, 2000
7. Jurgen Zemmer, Dietmar Knipp, Helmut Stiebig, and Heribert Wagner, "Amorphous silicon-based unipolar detector for color recognition", Vol.46, No.5 May 1999, IEEE Transactions on Electron Device
8. J.E. Laming and A. Martino, "Pc color recognition using led and software techniques", Vol.5, No.5, May 1993, IEEE Transactions on Electron Device
9. Shashi D. Buluswar, "color recognition in outdoor images". Department of Computer Science, University of Massachusetts, and Bruce A. Draper, Department of Computer Science, Colorado State University, 1997
10. Paul M. Zavracky and Erwin Hennenberg, "Miniature fabry perot spectrometers using micromachining technology", Northeastern Unversity, Department of Electrical and Computer Engineering, Boston, Massachusetts, 1999

11. M Stoksik. D T Nguyen. M Czernkowski, "A neural net based color recognition system", University of Tasmania, Austrilia, 1995

12. Frankie Y.C. Leung and M.S. Demokan, " Fiber-optic color sensor", Department of Electrical Engineering, Hong Kong Polytechnic University, 1997

13. Product information, "Rapid color recognition with compact 3-element color sensor", MAZeT, Gmbh, 2003, PI-99-036e V1.0

14. J.F.James and R.S.Sternberg, "The design of Optical Spectrometers", Lectures in Physics in the University of Manchester

15. Lijun Zhang and Mojtaba Kahrizi, "A new type of micro planar device for color recognition",11th Eleventh Canadian Semiconductor Technology Conference, Ottawa, Aug. 2003

16. H. L. Garvin, J.E.Kiefer, Hughes Research Lab, Mlibu, Calif. 90265, and S.Somekh, Calif. Institute of Technology, Pasadena, Calif. "Wire Grid Polarizers for 10.6μm Radiation",1976

17. J.B. Young, H.Z.Graham, and E.W.Peterson, "Wire grid infrared polarizer", Vol. 4, No.8, Applied Optics, 1965

18. Private Line Report on Projection Display; "Focus: Doing it with stripes" Vol. 7, No.10, April 20, 2001

Appendix 1

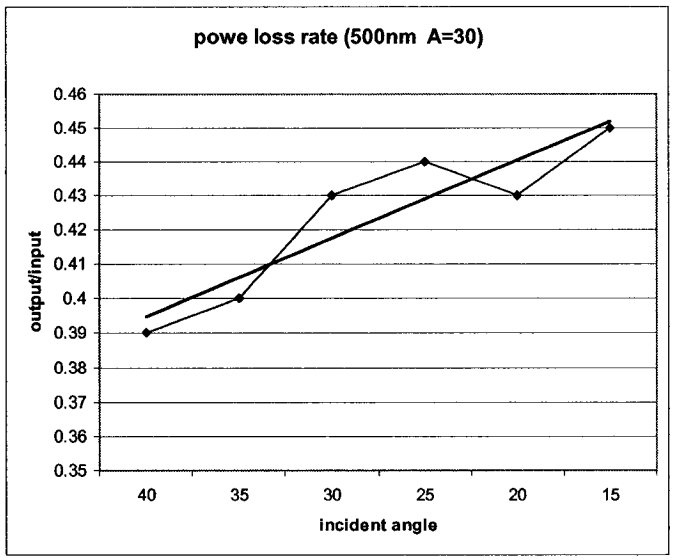

Figure A0 Waveform of power loss rate when A=30

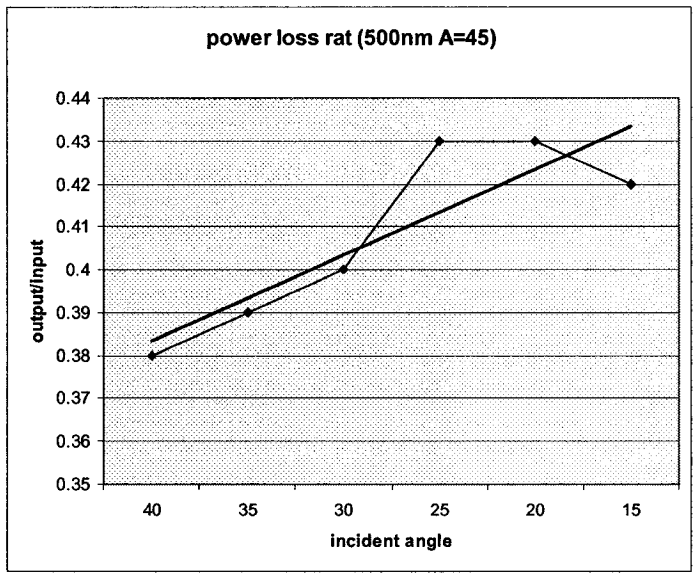

Figure A1 Waveform of power loss rate when A=45

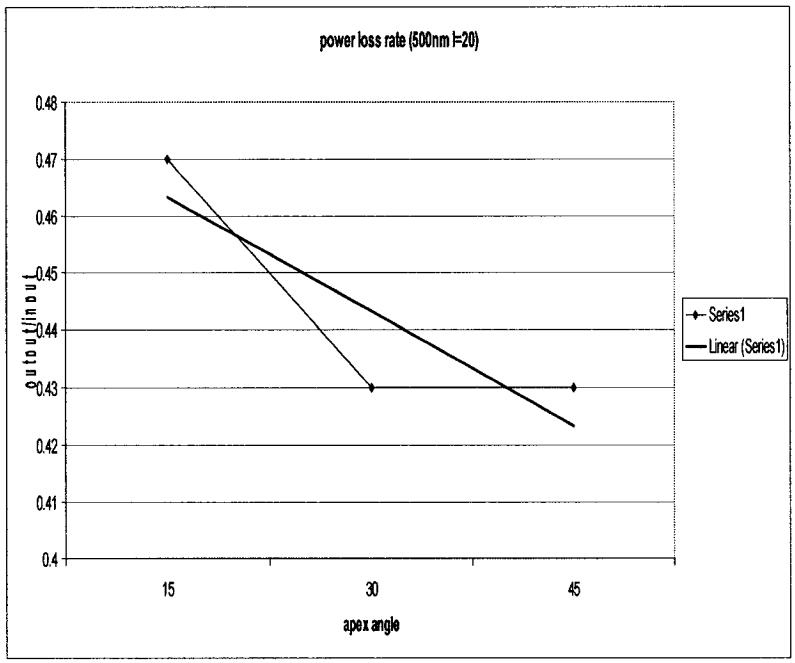

Figure A2 Waveform of power loss when I=20

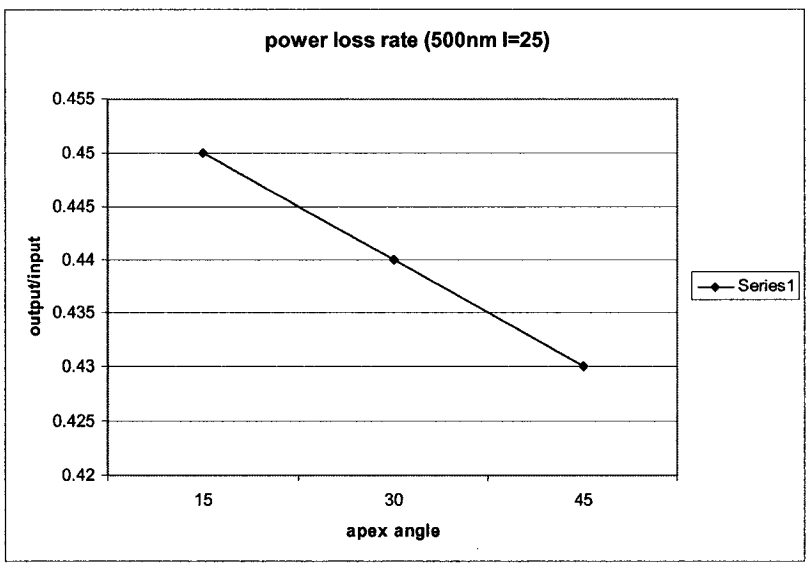

Figure A3 Waveform of power loss when I=25

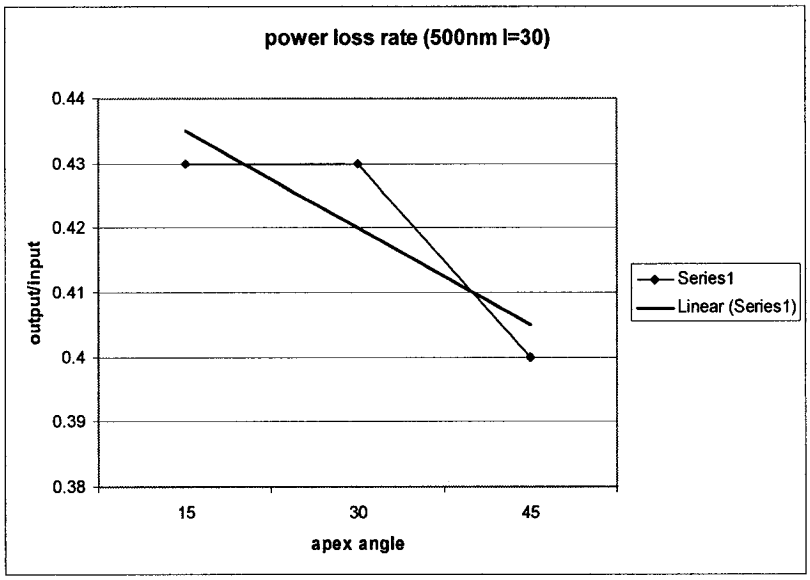

Figure A4 Waveform of power loss when I=30

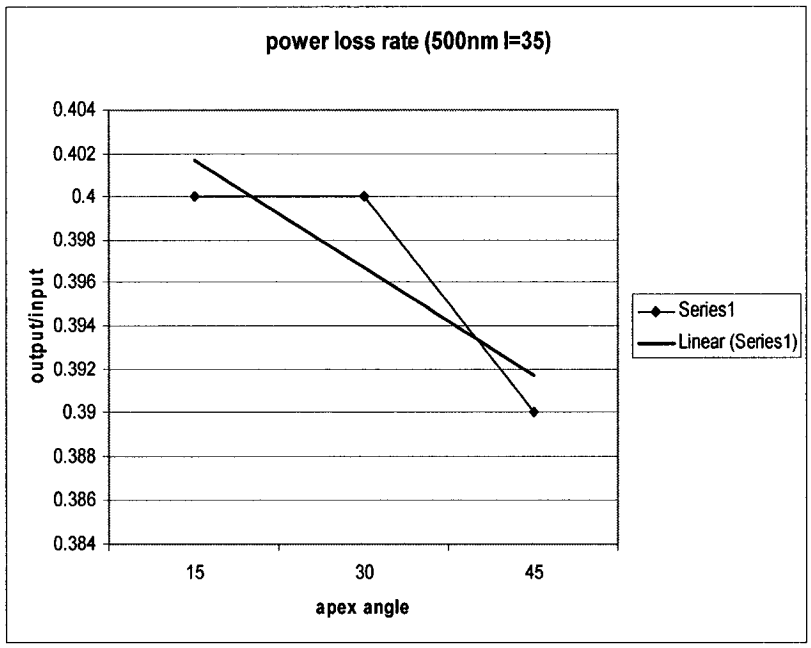

Figure A5 Waveform of power loss when I=35

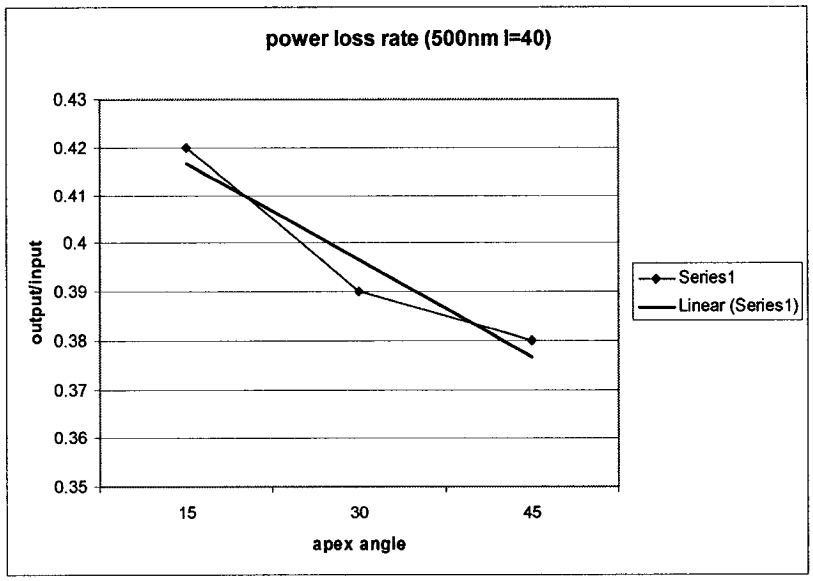

Figure A6 Waveform of power loss when I=40

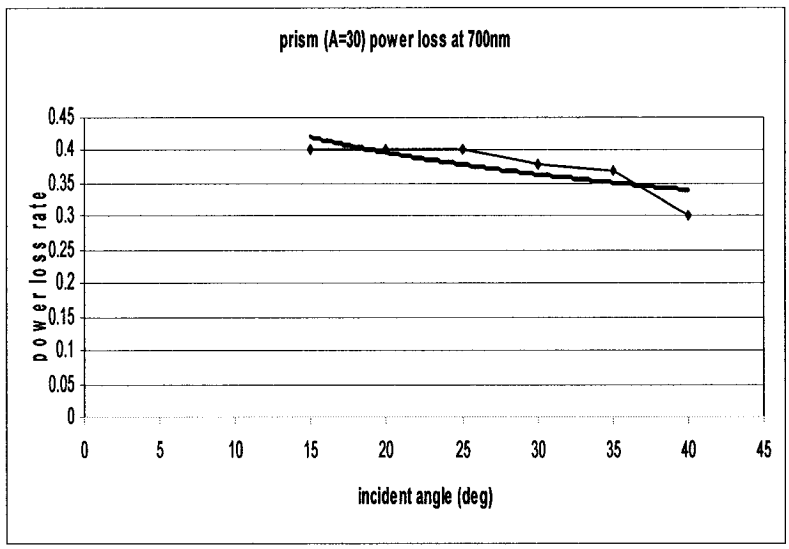

Figure A7 Waveform of power loss rate when A=30 deg

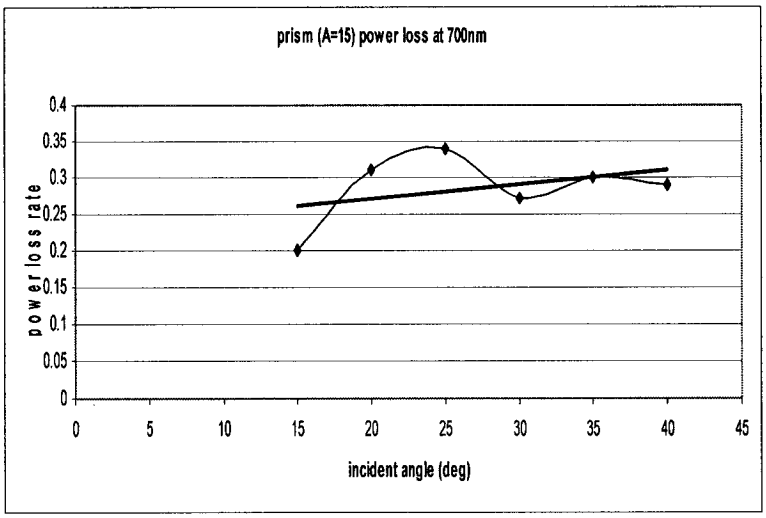

Figure A8 Waveform of power loss rate when A=15 deg

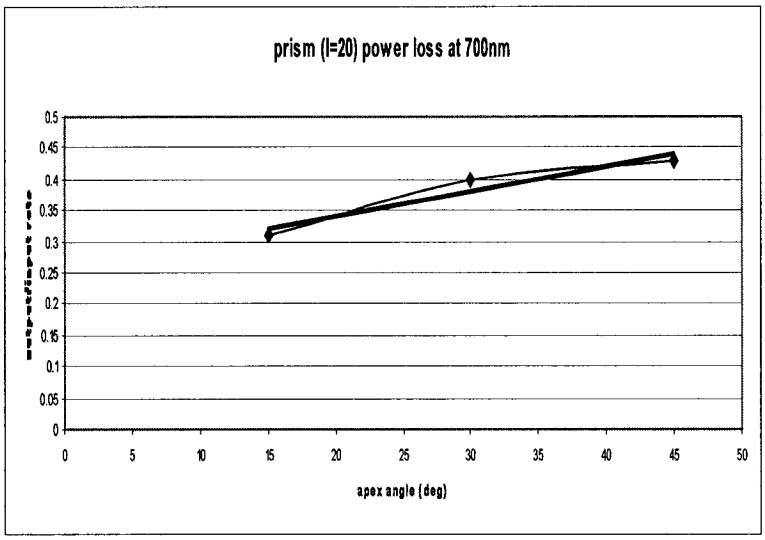

Figure A9 Waveform of power loss rate when A=20 deg

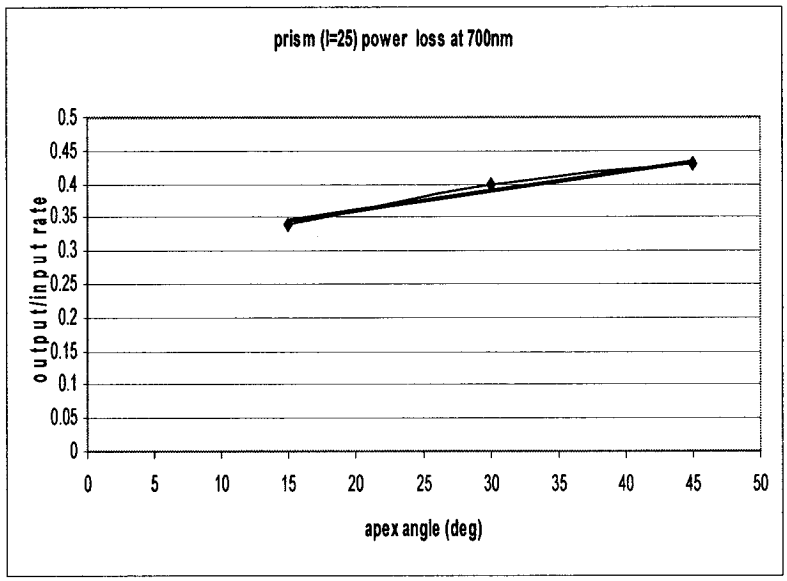

Figure A10 Waveform of power loss rate when A=25 deg

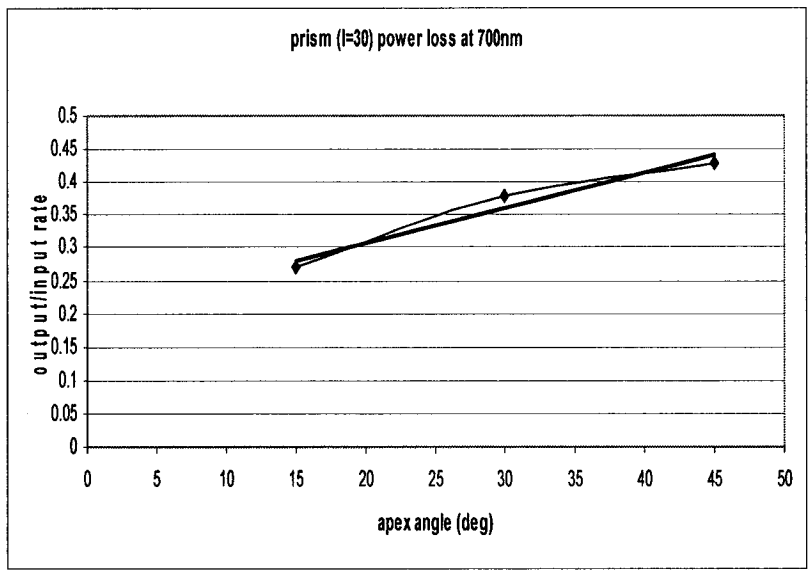

Figure A11 Waveform of power loss rate when I=30 deg

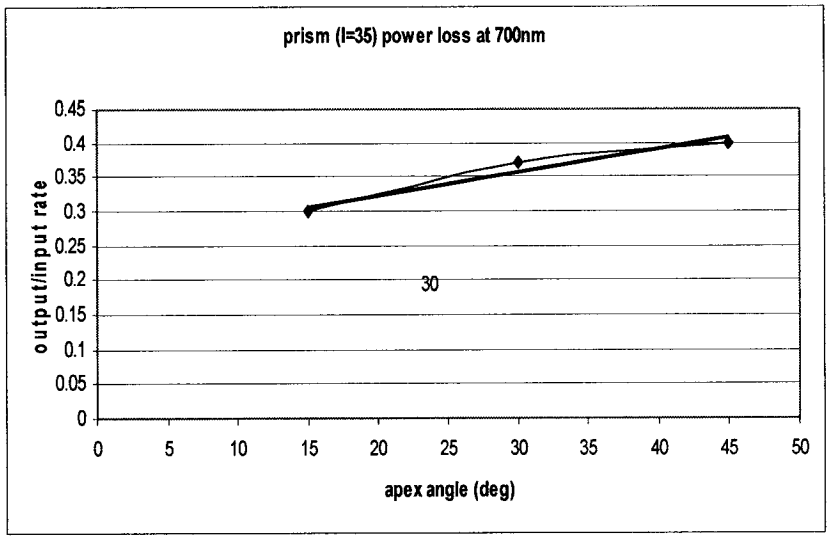

Figure A12 Waveform of power loss rate when I=35 deg

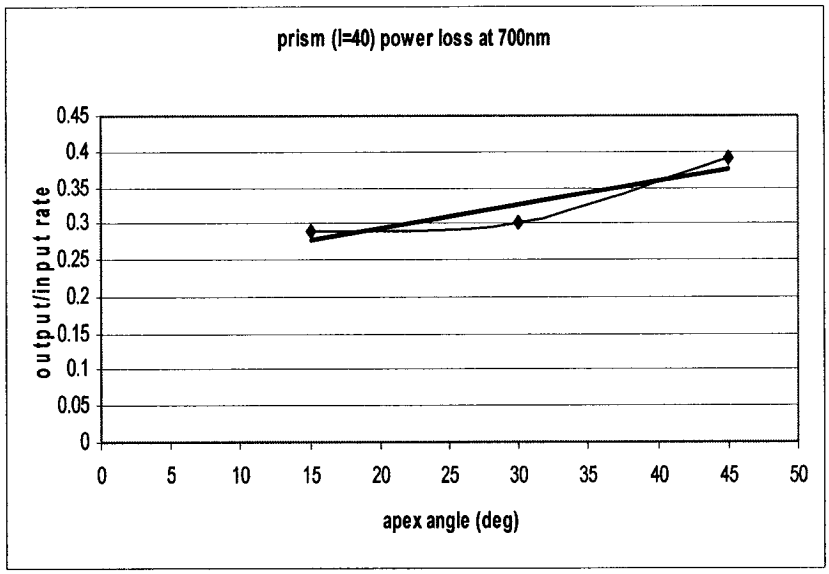

Figure A13 Waveform of power loss rate when I=40 deg

Appendix 2

Programming for lens

- For the relation of focus length vs lens' thickness, refer to the following figure and appendix 2.

The program for getting the diagram of parameters relation is below

```
%two variables
 step =1,n=1.377;
 for r1=50:5:70; r2=-r1
 for t=10:step:40
f = 1.0 / ( (n-1) * (1/r1 - 1/r2 + (n-1)*t / (n*r1*r2)) );
% f = 1.0 / ((n-1)*t/(n*r1*r2));
ezplot(f,[t t+step]);
hold on;
end
text(t,f,strcat('r1=',num2str(r1)))
end
```

- For relation between focus length vs refractive index, refer to appendix 2

```
%two variables
 step=0.001,t=30;
 for r1=50:5:70; r2=-r1
 for  n=1.350:step:1.500
f = 1.0 / ( (n-1) * (1/r1 - 1/r2 + (n-1)*t / (n*r1*r2)) );
% f = 1.0 / ((n-1)*t/(n*r1*r2));
ezplot(f,[n n+step]);
% focus with regard to refractive index
```

```
  hold on;
  end
  text(n,f,strcat('r1=r2=',num2str(r1)))
end
```

Appendix 3

- Following figure shows the relation between the incident angle and the deviation angle. Refer to appendix 3 for the calculation.

```
%multi-curves of prism deviation angle
n=1.377; l=asin(1/n);for a=0:.5:l
for x=0:0.1:1.55;y=x+asin(n*sin(a-asin(sin(x)/n)))-a;
% a is the value of apex angle, x is the incident angle. Y is the deviation
angle between the incident ray of light and the dispersed ray of light.
hold on;
  plot(x,y,'*')
end
hold on
end
```

Appendix 4

Calculation of change rate of reflected angle with respect to incident angle

```
a=30;r=10;step=.005;max=acos(r/a)
for p=0:step:max;   f=(a^2-a*r*cos(p))/(a*r*cos(p)-r^2);
ezplot(f,[p,step+p]),
hold on
end
```